Dietary and Microbial Oxazoles Induce Intestinal Inflammation by Modulating Aryl Hydrocarbon Receptor Responses

Iyer, Shankar S.; Gensollen, Thomas; Gandhi, Amit; Oh, Sungwhan F.; Neves, Joana F.; Collin, Frederic; Lavin, Richard; Serra, Carme; Glickman, Jonathan; de Silva, Punyanganie S. A.; Sartor, R. Balfour; Besra, Gurdyal; Hauser, Russell; Maxwell, Anthony; Llebaria, Amadeu; Blumberg, Richard S.

DOI:
10.1016/j.cell.2018.04.037

Dietary and Microbial Oxazoles Induce Intestinal Inflammation by Modulating Aryl Hydrocarbon Receptor Responses

Shankar S. Iyer[1], Thomas Gensollen[1], Amit Gandhi[1], Sungwhan F. Oh[2], Joana F. Neves[1], Frederic Collin[3], Richard Lavin[4], Carme Serra[5], Jonathan Glickman[6] Punyanganie S. A. de Silva[7], R. Balfour Sartor[8], Gurdyal Besra[9], Russell Hauser[10], Anthony Maxwell[11], Amadeu Llebaria[5], Richard S. Blumberg[1,12]

[1]Division of Gastroenterology, Hepatology and Endoscopy, Department of Medicine, Brigham and Women's Hospital, Harvard Medical School, Boston, Massachusetts USA.

[2]Department of Microbiology, Harvard Medical School, Boston, Massachusetts USA.

[3]Inspiralis Ltd., Innovation Centre, Norwich Research Park, Colney Lane, Norwich NR4 7GJ. UK.

[4]Center for Clinical and Translational Metagenomics, Department of Pathology, Brigham and Women's Hospital, Harvard Medical School, Boston, MA.

[5]Laboratory of Medicinal Chemistry, Department of Biomedicinal Chemistry, Institute of Advanced Chemistry of Catalonia IQAC–CSIC, Barcelona, Spain.

[6]Department of Pathology, Beth Israel Deaconess Medical Center, Boston, MA, USA.

[7]Division of Gastroenterology, Hepatology and Endoscopy, Brigham and Women's Hospital, Boston, Massachusetts.

[8]Departments of Medicine, and Microbiology and Immunology, University of North Carolina at Chapel Hill School of Medicine, Chapel Hill, North Carolina USA.

[9]School of Biosciences, University of Birmingham, Birmingham, United Kingdom.

[10]Department of Environmental Health, Harvard School of Public Health, Boston, Massachusetts, USA.

[11]Department of Biological Chemistry, John Innes Centre, Norwich Research Park, Norwich, NR4 7UH, United Kingdom.

[12]Correspondence: rblumberg@bwh.harvard.edu

Summary

Genome-wide-association-studies have identified risk loci associated with the development of Inflammatory Bowel Disease while epidemiological studies have emphasized that pathogenesis likely involves host interactions with environmental elements whose source and structure need to be defined. Here, we identify a class of compounds, derived from dietary, microbial and industrial sources that are characterized by the presence of a 5-membered-oxazole-ring and induce CD1d-dependent intestinal inflammation. We observe minimal oxazole structures modulate natural killer T cell dependent inflammation by regulating lipid antigen presentation by CD1d on intestinal epithelial cells (IEC). CD1d-restricted production of interleukin 10 by IECs is limited through activity of the aryl hydrocarbon receptor (AhR) pathway in response to oxazole induction of tryptophan-metabolites such that depletion of the AhR in the intestinal epithelium abrogates oxazole-induced inflammation. In summary, we identify environmental derived oxazoles as triggers of CD1d-dependent intestinal inflammatory response that occur via activation of the AhR in the intestinal epithelium.

Keywords

Inflammatory Bowel Disease; invariant natural killer T cell; mucosal inflammation; microbiota; microcin; oxazole; aryl hydrocarbon receptor; CD1d; intestinal epithelial cell; tryptophan; indoleamine 2,3 dioxygenase.

Introduction

Inflammatory bowel disease (IBD) is a complex disorder that evolves from the interactions between poorly understood environmental factors and a host's genetic framework that together define susceptibility to and severity of disease. Pathology is influenced by specific host elements that include the autochthonous commensal microbiota, which is acquired at birth, the intestinal epithelial cell barrier and subjacent immune cells within the intestinal mucosa (Kaser et al. 2010). One of the great challenges of understanding IBD pathogenesis stems from efforts to elucidate the molecular details surrounding the environmental basis for these disorders (Kaplan and Ng 2017). This is increasingly important since epidemiologic studies have revealed a rapid global expansion of these diseases that includes geographic regions, which have heretofore been unaffected (Molodecky and Kaplan 2010).

A potential opportunity to investigate this question has emerged from recent studies on the role of CD1d and natural killer T cells (NKT) in mucosal biology. CD1d is a nonpolymorphic, major histocompatibility complex (MHC) class I-related molecule in non-covalent association with β2-microglobulin that presents cell associated and microbial lipid antigens to NKT cells (Barral and Brenner 2007). In the intestines, CD1d is expressed by parenchymal cells, such as the intestinal epithelial cell (IEC), and hematopoietic cells such as professional antigen presenting cells (APC) residing in the lamina propria (Brigl and Brenner 2004, RossJohn et al. 2012, Van de waal et al 2003, Colgan et al. 1999, Dougan et al. 2007). CD1d-bearing IEC and APC present endogenous (self) or exogenous lipid antigens to NKT cells expressing an invariant T cell receptor (TCR) α chain (iNKT cells) or a semi-diverse (d) set of TCR-α chains (dNKT), which are present in human and mouse intestines (Brennan et al. 2013).

Both types of NKT cells have been implicated in the pathogenesis of IBD through studies of human tissues and an experimental mouse model of IBD involving the chemical induction of colitis using a classic chemical hapten, oxazolone (Wirtz et al. 2007). Boirevant and colleagues

first demonstrated that administration of oxazolone directly to the colon in ethanol of SJL/J mice, or in later studies indirectly after skin painting and sensitization suggesting a model of haptenization, resulted in a severe acute, superficial inflammation due to the production of interleukin (IL)-4 and IL-13 that was counter-balanced by tumor growth factor-β which delimited the inflammation to the distal colon (Boirevant et al. 1998). This restriction to type 2 cytokines was eventually recognized to be genetically based as similar studies in C57Bl/6 mice revealed inflammation in association with oxazolone that was due to type 1 cytokines (namely interferon-γ) derived from hematopoietic cells (Olszak et al. 2014, Iijima et al. 2004). In later groundbreaking studies by Heller and colleagues, it was recognized that oxazolone-induced colitis was dependent upon CD1d and iNKT cells as an inflammatory response to oxazolone was abrogated by the deletion of *Cd1d* or *Jα18*, encoding the invariant TCR-α chain (Heller et al. 2002). Moreover, the pro-inflammatory effects of CD1d-iNKT cell interactions in response to oxazolone were primarily derived from the activity of professional APC in the lamina propria using bone marrow chimeras (Olszak et al. 2014). In contrast, CD1d-expressing IECs were shown to secrete anti-inflammatory IL-10 in response to iNKT cells in a CD1d-dependent manner, which serves to restrain oxazolone-induced inflammation derived from the hematopoeitic system (Colgan et al. 1999, Olzsak et al. 2014). As such, when CD1d-restricted pathways in the IEC are specifically eliminated by conditional genetic deletion of *Cd1d*, microsomal triglyceride transfer protein (*Mttp*), an endoplasmic reticulum resident protein which serves to regulate CD1d lipidation and its ability to function, or *Il10*, oxazolone-induced colitis is unrestrained and severe (Dougan et al. 2005, 2007, Sagiv et al. 2007, Olszak et al. 2014). Human studies have further identified a potential role for dNKT cells in IBD by showing elevated IL-13 production by lamina propria mononuclear cells in response to sulfatide, a CD1d-restricted self-antigen which can activate iNKT and dNKT cells (Fuss et al. 2004, Fuss et al. 2014). Further, T cell receptor (TCR) transgenic mice expressing a non-invariant CD1d-restricted TCR

develop colitis (Wang et al. 2017). Moreover, some studies have shown that T cells expressing Vα24, the TCRAV chain expressed by iNKT cells, are increased in the intestinal mucosa and blood of patients with IBD; although others have reported the opposite observations suggesting a decrease of TCRAV bearing cells or their receptor upon activation (Fuss et al. 2004, Grose et al. 2007, van der Vliet et al. 2001). These studies together suggest that NKT cells may play a role in the pathogenesis of IBD.

Importantly, these host inflammatory responses to oxazolone occur even in animals raised under germ free (GF) conditions, indicating that NKT cell mediated response to self (rather than microbial) lipid antigens presented by CD1d on professional and/or non-professional antigen presenting cells (APC) is sufficient for pathogenesis (Olszak et al. 2012). Instead, commensal bacteria themselves can modulate the magnitude of NKT cell responses either by directly altering the CD1d-restricted lipid antigen reservoir (An et al. 2014, Wieland Brown et al. 2013) or indirectly by regulating the quantity of iNKT cells in the colon (Olszak et al. 2012). In the latter case, the absence of appropriate microbial signals in early life leads to elevated levels of iNKT cells in the colon that in later life makes the host susceptible to the colitogenic effects of oxazolone (Olszak et al. 2012). Conversely, CD1d itself plays a critical role in regulating the composition and extent of colonization by both commensal and pathogenic microbial species potentially through disruption of the anti-microbial activity of Paneth cells (Nieuwenhuis et al. 2005, Nieuwenhuis et al. 2009, Farin et al. 2014).

The similarities between these biological observations in mouse models and current hypotheses for IBD pathogenesis wherein environmental triggers activate inflammation in a susceptible host lead us to hypothesize that oxazolone may be an example of a much larger collection of environmental chemical moieties capable of triggering CD1d-restricted iNKT cell responses. Consistent with this, we observe an abundance of oxazolone-related chemicals in the environment and microbiota capable of inducing intestinal inflammation. Specifically, we

have identified environmental mimetics of oxazolone that are derived from dietary, industrial or microbial sources which are characterized by the presence of a 5-membered oxazole ring and capable of driving CD1d-dependent inflammation through activation of the aryl hydrocarbon receptor pathway within IECs of the colon. As efforts to define and evaluate natural and synthetic chemicals involved in homeostasis or disease have generally been elusive, these results have broad implications for understanding the environmental basis of mucosal diseases such as IBD.

Results

Defining a structural moiety that modulates epithelial derived CD1d dependent inflammatory responses.

4-ethoxymethylene-2-phenyl-2-oxazol-5-one, (referred to as oxazolone, Fig. 1A) has been widely utilized in models of contact hypersensitivity and when applied to the mucosa has been proposed to cause colitis through its properties as a hapten (Gorbachev and Fairchild 2001). However to date there is limited evidence for hapten-specific antibody production or responses following topical oxazolone sensitization or hapten modified autologous proteins or luminal antigens identified at mucosal sites (Singleton et al. 2016, Yanaba et al. 2008, Wirtz et al. 2007). Interestingly, upon analysis of previously published microarray studies derived from epithelial enriched colon fractions following intra-rectal oxazolone challenge (Olszak et al. 2014), we observed decreased transcripts for microsomal triglyceride transfer protein (*Mttp*, MTP) and increased transcripts for elements associated with aryl hydrocarbon receptor (AhR) signaling, including P450 enzymes (*cyp1a1*) and indoleamine 2,3-dioxygenase (*Ido1*). We therefore asked whether oxazolone could affect the expression of these transcripts in the intestinal epithelium in a cell intrinsic manner by directly stimulating an immortalized intestinal epithelial cell line (IEC) derived from mouse small intestine, MODE-K, with oxazolone. We observed down-regulation of *Mttp* and induction of metabolic genes *cyp1a1* and *Ido1* (Fig. 1B, S1A).

MTP is a critical regulator of mucosal homeostasis that promotes epithelial barrier activity by controlling CD1d-restricted IL-10 production by epithelial cells (Colgan et al. 1999, Olszak et al. 2014). Thus IEC specific deletion of *Mttp* results in decreased CD1d-stimulated IL-10 production by the IEC leading to the exaggerated inflammatory activity of hematopoietic cells in response to oxazolone challenge resulting in increased colitis (Olszak et al. 2014). We therefore modeled interactions between NKT cells and IECs using MODE-K cells and CD1d-restricted T cell hybridomas in a previously described CD1d-dependent co-culture system (van de Wal et al. 2003). These studies have shown that loading of CD1d with alpha-galactosyl ceramide (α-GC), a cognate lipid antigen, in this co-culture system, leads to MTP-dependent, CD1d-restricted IL-10 production that is primarily derived from the IEC (Brozovic et al. 2004, Colgan et al. 1999, Olzsak et al. 2014). Here, we found that MODE-K cells pre-conditioned with oxazolone exhibited attenuated IL-10 production in response to α-GC when placed in co-culture with an iNKT cell hybridoma (24.7), which specifically reacts to α-GC presented on CD1d (Fig. 1C). Interestingly, epithelial derived IL-10 was also suppressed when IECs pre-conditioned with oxazolone were co-cultured with an autoreactive iNKT cell hybridoma (24.8) or an autoreactive non-invariant dNKT cell hybridoma (14S.6) in the absence of exogenously administered α-GC (Fig. S1B, S1C). These effects were specific to the IEC as co-culture of bone marrow-derived dendritic cells with the 24.7 iNKT cell hybridoma and α-GC lead to production of IFN-γ (Fig. S1D) but not IL-10 (data not shown) which was not affected by oxazolone or any of the oxazolone-related compounds described below.

In light of the decreased MTP expression observed in oxazolone treated IECs (Fig. 1B) and given that MTP loss alters the ability of CD1d to acquire exogenous antigens, such as α-GC, and CD1d elicited IL-10 responses by epithelial cells (Dougan et al. 2005, Dougan et al. 2007, Zeissig et al 2017, Sagiv et al. 2007, Brozovic et al. 2004, Olszak et al. 2014), we

investigated CD1d expression and lipid loading on oxazolone conditioned IECs. IECs stimulated with oxazolone did not display altered CD1d protein expression or distribution between intracellular and cell surface pools (Fig. S2A, S2B), but instead exhibited decreased loading of α-GC on CD1d at the cell surface based upon staining with the CD1d-α-GC complex specific monoclonal antibody (L363) which revealed decreased mean fluorescence intensity on IECs exposed to oxazolone (Fig. 1D, 1E). These results were consistent with the decreased CD1d-restricted IL-10 protein production we observed in MODE-K:iNKT cell co-cultures (Fig.1C, S1B, S1C), and suggest that oxazolone induced alterations in MTP expression were associated with decreased CD1d function affecting IL-10 production in response to iNKT cells, supporting previous observations of MTP activity in IEC (Dougan et al. 2005, Dougan et al. 2007).

Oxazolone is administered in experimental models of colitis and contact sensitivity but is also widely used in industry and pharmaceuticals as a pharmacophore for the generation of synthetic compounds suggesting it may act as a potential environmental trigger of inflammation in sensitive hosts (Turchi 2008). We therefore sought to identify a library of structural mimetics of oxazolone and test whether these molecules behaved in a similar manner. We performed a two part *in silico* screen against three chemical databases of naturally occurring compounds (Human Metabolome Database, Super Natural II database, Dictionary of Natural Products) (Banerjee et al. 2015, Wishart et al. 2007) thereby limiting our search to compounds within a defined human envirome. Natural compounds were queried in the standard SMILES format and Tanimoto similarities between oxazolone and test compounds were computed with the ChemMine Similarity Workbench, which calculated maximum common substructure (MCS) similarities with the Tanimoto coefficient. Further, Euclidean distance scores were calculated using a non-continuous atom matching structural similarity function (NAMS) (Cao et al. 2008, Teixeira et al. 2013). An initial screen identified 33 compounds with MCS >0.5 and Euclidean distance scores cutoff of 0.9 (Table S1). Oxazolone consists of four major functional moieties: a 5-membered oxazole ring, a 2' phenylgroup, a 4' ethoxymethylene substituent, and the 5'-

carbonyl lactone. Our computational screen revealed the oxazole ring to be a distinctive and shared chemical sub-structure between the 33 compounds identified, all of which derived from dietary, microbial and/or industrial sources. We then employed a second screen using the same parameters but instead substituting a minimal oxazole ring as our template structure. The analysis led to the identification of 63 naturally occurring oxazole-containing (OxC) compounds (including the 33 described above), Of particular interest, we noticed that many of these compounds derived from three major sources: diet, microbes, and agriculture. This led us to determine whether oxazolone is a molecular prototype for a broader class of environmental stimuli that feature an oxazole sub-structure capable of modulating epithelial CD1d-restricted responses in a cell intrinsic manner.

To test this, we devised a systematic *in vitro* system to assess transcriptional and CD1d-restricted responses in IECs in response to stimulation with dietary OxC structures, including 2,4,5-trimethyl-2,5-dihydro-1,3-oxazole (referred to as TMO, Fig. 1A) found in coffee, peanuts, meats and utilized as a food additive, which lacks the 2-phenyl ring, 5-ketone, and 4-ethoxymethylene present in oxazolone (Vitzthum et al. 1975, Stoffesima et al. 1968, Lee et al. 1981, Chang et al. 1968, Ho and Hartman 1968). Like oxazolone, TMO suppressed *Mttp* and induced *cyp1a1* and *Ido1* transcripts in IECs (Fig. 1B, S1). In contrast two structurally related non-OxC heterocyclic aromatic compounds 1,2,4-trimethyl cyclopentane (MCS=0.5, referred to as TMC) and 2-methyl-1-pyrroline (MCS=0.83, referred to as 1-MP), that substitute carbons at the 1'-oxygen and/or 3'-nitrogen, did not elicit any transcriptional changes in the target genes assessed (Fig. 1B). Moreover, IECs conditioned with oxazolone or TMO but not TMC or 1-MP limited CD1d-restricted IL-10 production in co-cultures with an iNKT hybridoma (24.7) and the ability of CD1d to be lipidated with exogenously administered α-GC as revealed by decreased cell surface staining with the L363 monoclonal antibody (Fig. 1C, 1D, 1E). Overall, 5 of 7 tested naturally occurring dietary OxC as well as vinclozolin (Fig. 1A), an OxC fungicide used in

agriculture, phenocopied the transcriptional and CD1d-restricted epithelial responses observed after oxazolone stimulation.

A minimal oxazole structure induces colonic inflammation in a CD1d dependent manner.

We next asked if a dietary sourced minimal oxazole structure was sufficient to induce intestinal inflammation *in vivo*. Indeed intra-rectal administration of TMO was observed to lead to increased weight loss, colon shortening, and histological pathology characterized by superficial inflammation of the gut wall, neutrophil accumulation and ulceration of the epithelial layer of the colon that was similar to the inflammation associated with oxazolone (Fig. 1F, 1G, S3A) (Heller et al. 2002). The immune response to TMO but not 1,2,4-trimethylcyclopentane (TMC) or vehicle was characterized by production of Th2 and Th1 cytokines including IL-13 and IFN-γ from colon explants consistent with the genetic background of the hosts, C57Bl/6 (Fig. 1H) (Iijima et al. 2004). Importantly, intestinal inflammation after TMO challenge was dependent on the presence of iNKT cells, as CD1d-deficient animals displayed no evidence of clinical symptoms or pathology (Fig. 1F, 1G) as previously shown for oxazolone (Boirevant et al. 1998, Heller et al. 2002). In addition, the host *in vivo* IEC responses to TMO but not TMC or vehicle recapitulated the transcriptional changes observed in microarray and *in vitro* analyses including downregulation of *Mttp* and induction of *cyp1a1* (Fig. S3B, S3C). Importantly, these studies were performed by direct administration of TMO to the colonic epithelium by rectal challenge without preceding skin sensitization further suggesting that the OxC-induced effects observed were direct and did not require prior immune activation as would be expected from a hapten-induced model. To confirm this, we compared the ability of oxazolone skin pre-sensitization to affect the responses to rectal challenge with TMO and vice-versa (Fig. S3D). These studies showed that pre-sensitization with oxazolone or TMO did not affect rectal responses to TMO or oxazolone, respectively; providing further evidence that oxazolone or TMO were having direct effects on the colonic mucosa.

A microbial derived oxazole structure modulates epithelial responses and leads to intestinal inflammation.

Our *in silico* analysis also identified a class of bacterial derived toxins featuring oxazole moieties with a high degree of similarity to a minimal oxazole template. These are termed thiazole/oxazole modified microcins (TOMMs), a family of anti-microbial peptides featuring the presence of thiazol(in)e and oxazol(in)e heterocycles derived from cysteine, serine, and threonine residues on a ribosomally produced precursor peptide that confer a range of anti-microbial activities including DNA gyrase inhibitors, translation inhibitors and hemolytic toxins (Table S1) (Melby et al. 2011, Collin et al. 2013, Vizan et al. 1991, Lee et al. 2008, Sassone-Corsi et al. 2016). Though chemically and functionally diverse, as a rule TOMM biosynthetic gene clusters encode a leader peptide, enzymatic machinery including a cyclodehydratase and cyclodehydrogenase, that mediate post-translational installation of oxazole/thiazole moieties required for biological activity, and in some cases an immunity gene that protects the host strain from the anti-microbial activities of the TOMM itself (Melby et al. 2011). Importantly, many TOMM biosynthetic gene clusters (BGC) have been described in a variety of human commensal communities as a means of providing host strains with ecological fitness advantages (Donia et al. 2014, Lee et al. 2008, Sassone-Corsi et al. 2016). Within the commensal populations, these BGC encoded small molecule bacterial signaling factors collectively have an enormous potential to mediate microbe-microbe interactions (Donia et al. 2014, Wyatt et al. 2010, Nougayrede et al. 2006, Mazmanian et al. 2005, 2008, An et al. 2014, Wieland-Brown et al. 2013, Yoshimoto et al. 2013). Therefore, we considered it possible that microcins also regulated microbe-host interactions. We therefore asked whether oxazole containing microcin products modulated epithelial derived CD1d immune responses in the host as did other OxC compounds. To address this question, we focused our attention on Microcin B17 (MccB17, MCS=0.75), originally isolated from strains of *Escherichia coli* (*E. coli*) from the intestinal tract of newborns whose expression is linked to a plasmid (pMccB17) that carries a 7 gene *mcb* operon, encoding

the MccB17 toxin that acts as a DNA gyrase inhibitor (Table S1, Yorgey et al. 1994, Li et al. 1996). The *mcb* operon was previously cloned into a pUC19 vector (Collin et al. 2013) and transformed into a competent *E. coli* BSL1 human commensal strain (*MG1655*). MccB17 production is induced by growing bacteria in nutrient rich M63 media (Collin et al. 2013). Bacteria transformed with *mcb17* or empty plasmid was grown in Luria Broth or M63 supplemented media and bacterial lysates incubated with IECs after which we measured CD1d-restricted responses upon co-culture with an iNKT cell hybridoma. We observed that lysates from bacterial isolates transformed with *mcb* and grown under MccB17 permissive conditions, but not non-transformed bacteria, attenuated CD1d-restricted IL-10 production in MODE-K:iNKT cell co-cultures, whereas lysates isolated from bacteria grown under non-permissive conditions or transformed with empty plasmid had no effect (Fig. 2A). To further examine whether suppression of CD1d-restricted responses was due to a MccB17 product, full length mature MccB17 was purified by High Performance Liquid Chromatography (HPLC) and examined in the aforementioned IEC:iNKT co-culture assay. To our surprise, purified MccB17 exerted no effects on CD1d dependent IL-10 production (Fig. 2B). However, although the full length MccB17 microcin consists of a 3093 Da peptide, several smaller heterocyclic *mcb17* derived heterocyclic species have been identified by MALDI-ToF mass spectrometry analysis which may or may not retain DNA gyrase inhibitory activity suggesting that the immunomodulatory effects of the MccB17 positive lysate might be a result of proteolytic and/or degradative products rather than the mature full length MccB17 itself (Collin et al. 2013, Sinha Roy et al. 1998). B17 microcin is sensitive to cleavage by subtilisin but not trypsin (Asensio and Perez-Diaz 1976). Therefore, we digested purified full length B17 with each protease and measured CD1d-restricted IL-10 responses in the IEC:iNKT cell co-culture assay to these proteolytic products (Fig. 2B). In this case, cleavage products from subtilisin but not trypsin were able to attenuate IL-10 production in IEC:iNKT co-cultures with α-GC. Similarly, we observed decreased *Mttp* and induction of

Cyp1a1 transcripts in MODE-K cells incubated with MccB17 subtilisin proteolytic products but not full length B17 or MccB17 digested with trypsin (Fig. 2C).

Taken together, these results suggested that the ability of MccB17 derived toxins to affect epithelial transcriptional and CD1d-restricted responses is limited by the size of the product. To clarify this size restriction, we screened a library of 8 synthetic MccB17 derived products with molecular weights ranging from 183.17-857.82 Da that are analogous to naturally produced MccB17 fragments and whose anti-DNA gyrase activity has been previously described (Fig. 2D) (Collin et al. 2013). Consistent with our hypothesis, four fragments, containing permutations of 1 or 2 oxazole/thiazole moieties, with MW<270 Da were able to modulate CD1d dependent IL-10 production and regulate *Mttp* and *Cyp1a1* whereas synthetic products >500Da were not (Fig. 2E, 2F and data not shown). Importantly, synthetic analogs capable of exerting immunomodulatory effects were within the relative size range of both oxazolone (217.22 Da) and 2,4,5-trimethyl-2,5,-dihydro-1,3-oxazole (113.16 Da) but surprisingly even synthetic products that did not confer anti-DNA gyrase activity were able to generate epithelial responses (Fig. 2D, 2E, 2F). Furthermore, both oxazole and thiazole containing compounds generated similar effects consistent with their shared physico-chemical properties (Fig. 2D, 2E, 2F).

A synthetic B17 microcin derivative induces colonic inflammation in a CD1d-dependent manner independent of anti-microbial activity.

We next asked whether B17 microcin derivatives could induce intestinal inflammation *in vivo*. We therefore synthesized adequate quantities of a minimal B17 derivative (termed frag-oz, Fig. 2D) to perform *in vivo* experiments and challenged animals via intra-rectal administration. Like oxazolone and TMO, we observed CD1d-dependent pathology as well as induction of both Th1 and Th2 cytokines from colon explants suggesting that this molecule induces inflammation in an iNKT dependent manner as inflammation and hematopoietic cell derived cytokine responses could be observed in WT, but not *Cd1d*$^{-/-}$ (CD1d KO), mice (Fig. 3A, 3B, 3C, S3A). We also

observed decreased *Mttp* levels and induction of *Cyp1a1* in IEC enriched colonic fractions suggesting that frag-oz exerts immunomodulatory effects via the epithelial compartment *in vivo* (Fig. 3D. 3E). Though *in vitro* studies showed that frag-oz confers no anti-gyrase activity (Collin et al. 2013), to formally rule out the possibility that the intestinal inflammation observed was due to direct effects on the host rather than through its anti-microbial properties, we challenged GF and SPF mice with frag-oz or vehicle. Consistent with this, GF animals exhibited increased weight loss compared to animals raised under SPF conditions together with severe inflammation as defined by quantitative histopathology (Fig. 3C, 3F). These studies thus identify an oxazole containing microbial mimic that promotes CD1d-dependent intestinal inflammation independent of its classical anti-microbial activity.

Activation of epithelial aryl hydrocarbon receptor pathways exacerbates responses to dietary and microbial oxazole compounds by limiting IL-10 responses.

The data presented support a model in which exposure to a broad class of oxazole (or thiazole) ring containing compounds can direct transcriptional changes in responsive tissue compartments, such as the intestinal epithelium, that influence CD1d-restricted antigen presentation pathways resulting in compromised barrier integrity at mucosal sites, thereby augmenting iNKT (or non-invariant NKT) cell inflammatory responses, leading to colitis. These data also suggest the presence of cellular sensor(s) that are responsible for recognizing and transducing oxazole dependent signals. Review of our previous microarray analyses identified two signature aryl hydrocarbon receptor (AhR) targets, *cyp1a1* and *Ido1*, involved in P450 and tryptophan metabolism, respectively, as inducible gene targets in the colonic epithelium (Olszak et al. 2014). Here we demonstrate that oxazolone, vinclozin, an industrial agent, and the dietary and microbial oxazole ligands, TMO and frag-oz, induced expression of these genes *in vitro* and *in vivo*. Interestingly, vinclozolin, an antifungal agent to which humans are exposed through agriculture and which affects CD1d-restricted pathways as an OxC as shown here, has been described as an AhR activator (Wambaugh et al. 2014, Dierickx 2004).

We therefore transfected IECs with an AhR firefly luciferase reporter and observed that oxazolone, TMO and 5 additional dietary oxazoles, as well as 4 synthetic MccB17 derivatives induced robust AhR transcriptional activity compared to vehicle or a non-oxazole heterocyclic control, 1,2,4-trimethylcyclopentane (Fig. 4A). Consistent with this, siRNA mediated knockdown of AhR in MODE-K cells abrogated induction of *cyp1a1* and *IDO1* and partially restored *Mttp* expression (Fig. S4A-C). Given that AhR regulates MTP expression we asked whether this pathway could modulate epithelial derived CD1d-restricted responses. Indeed, AhR deficiency caused by silencing AhR expression in epithelial cells reversed oxazolone, TMO or frag-oz induced inhibition of CD1d-restricted IL-10 production in IEC:iNKT cell co-cultures and reduction of cell surface CD1d lipid antigen loading (Fig. 4B, 4C). This was confirmed in hepatocytes obtained from $Ahr^{-/-}$ mice, which also exhibited resistance to the effects of oxazolone, TMO, frag-oz or vinclozin induced inhibition of IL-10 production in response to iNKT cells in the presence of α-GC (Fig. S5). Interestingly, these effects were not attributed to general AhR function, but instead reflected a specific response to oxazole containing molecules as a human cognate AhR ligand, 2-(1*H*-Indol-3-carbonyl)-4-thiazolecarboxylic acid methyl ester (ITE), did not modulate *Mttp* expression or CD1d-restricted responses (Fig. 4B, 4C).

These studies reveal a novel role for epithelial derived AhR signals in promoting mucosal inflammation when exposed to OxC. Consistent with this hypothesis, deletion of *Ahr* specifically in IECs (generated by crossing $Ahr^{fl/fl}$ to Villin-Cre transgenic animals, $Ahr^{\Delta IEC}$) resulted in elevated IL-10 production in colonic explants after oxazolone or frag-oz compared to wildtype controls (Fig. 4D), and conferred host protection to oxazolone (Fig. 4E, 4F) and frag-oz (Fig. 4G, 4H) after intra-rectal challenge as characterized by diminished weight loss and disease manifestations relative to that observed in $Ahr^{fl/fl}$ mice.

Oxazoles induce the generation of tryptophan derived metabolites that attenuate epithelial CD1d-restricted responses in an AhR dependent manner.

Our studies show that although AhR regulates CD1d-restricted responses to oxazole containing compounds, this is not a property of all AhR ligands (such as ITE). This suggests that epithelial responses to OxC generate AhR agonists uniquely capable of attenuating IL-10 production through CD1d-restricted mechanisms. It was therefore of interest that we observed IDO1 upregulation in IECs exposed to oxazoles (Fig. S1A). IDO1 is a rate-limiting enzyme involved in tryptophan catabolism that generates formyl-kynurenine which can be further metabolized into a variety of AhR agonists (Higuchi and Hayaishi Arch Biochem Biophys 1967, Nguyen and Bradfield 2008, Zelante et al. 2014). Indeed, incubation of recombinant IDO1 with oxazolone, TMO or frag-oz enhanced the ability of IDO1 to convert tryptophan to formyl-kynurenine compared to control (TMC) or vehicle indicating that oxazole compounds may function to enhance IDO1 enzymatic activity through direct means (Fig. 5A). To test whether tryptophan metabolism is therefore involved in the AhR effects we observed, we cultured IECs in tryptophan-deficient media and found that CD1d-restricted IL-10 production was no longer attenuated by stimulation with oxazolone, TMO or frag-oz when compared to TMC or vehicle controls (Fig. 5B). On the other hand, supplementation with exogeneous L-tryptophan (L-Trp) restored responses to oxazolone, TMO and frag-oz resulting in attenuation of CD1d-restricted IL-10 production supporting a role for tryptophan-derived metabolites in this process (Fig. 5B). To specifically identify these tryptophan derived products, we cultured IECs with deuterated L-trp (D5-Trp) and performed high performance liquid chromatography mass spectrometry (LC-MS) on lysates stimulated with oxazolone, TMO, frag-oz or TMC control (Fig. 5C). We detected uptake of D5-Trp in TMC stimulated IECs that was further metabolized to kynurenic acid and 3-hydroxy kynurenic acid (referred to as xanthurenic acid) only upon stimulation with oxazolone or TMO and frag-oz, respectively, within 6 hours of exposure to oxazoles (Fig. 5C). To further

investigate whether tryptophan-derived metabolites attenuate CD1d-restricted responses, we cultured IECs in tryptophan-deficient media supplemented with L-Trp, kynurenic acid, xanthurenic acid, or an upstream tryptophan product, kynurenine, in the presence or absence of oxazolone. Supplementation with exogenous tryptophan or its downstream products of catabolism restored IEC responses to oxazolone as shown by reduced CD1d-restricted IL-10 production (Fig. 5D). In contrast, supplementation with DL-methyl tryptophan (DL-Mtrp) a tryptophan competitive inhibitor of IDO1, did not restore suppression of CD1d-restricted IL-10 production in IECs cultured in tryptophan-deficient conditions and stimulated with oxazolone (Fig. 5D). Finally, to ascertain whether these same metabolites identified in our LC-MS analyses, functioned through the AhR pathway, we performed siRNA-mediated knockdown of AhR in IECs cultured under tryptophan-deficient conditions in the presence of exogenously administered kynurenic acid and measured CD1d-restricted IL-10 production after stimulation with OxC compounds (Fig. 5E). Incubation of IECs with L-Trp or kynurenic acid alone or in conjunction with TMC stimulation had no effect on CD1d-restricted IL-10 production (Fig. 5B, 5D). In contrast, IECs cultured under tryptophan-deficient conditions and stimulated with oxazolone, TMO or frag-oz when supplemented with kynurenic acid led to decreased IL-10 production that was reduced when AhR was silenced (Fig. 5E). Taken together these latter studies are consistent with a model in which exposure of IECs to oxazole containing compounds leads to the activation of IDO1 and generation of tryptophan-derived metabolites that induce the AhR pathway to downregulate CD1d-restricted responses associated with the production of IL-10 (Fig. 6).

Discussion

In the studies described herein, we have used structural analyses of oxazolone, a compound previously shown to be capable of inducing inflammation of the colon (Boirevant et al. 1998, Heller et al. 2002, Dietrich and Hess 1970), to identify a new and potentially broad class of

dietary, microbial, and other environmental derived factors within the human exposome (Melby et al. 2011, Wambaugh et al. 2014, Donia et al. 2014, Asensio and Perez-Diaz 1976). As shown here, these compounds are capable of direct induction of intestinal inflammation through crosstalk of CD1d-restricted and aryl hydrocarbon receptor pathways in intestinal epithelial cells. These structures, which we name oxazole-containing compounds (OxC), include a variety of chemicals used in agriculture (e.g. vinclozolin), food additives and processing (e.g. TMO) and microbial factors (e.g. bacterial microcins). In the latter case, we demonstrate that in addition to their well-established role as anti-microbial peptides, bacterial microcins are capable of inducing host responses. Together, this suggests that environmental agents capable of activating CD1d-restricted pathways can do so by phenocopying host responses to microbial factors. In light of the wide presence of OxC in the environment including a number of microbial sources (Melby et al. 2011), these results have important implications for understanding potential environmental triggers that influence susceptibility to inflammation associated with the body surfaces associated with skin (e.g. dermatitis and contact hypersensitivity), intestines (e.g. IBD, allergy), esophagus (e.g. eosinophilic esophagitis), lungs (e.g. asthma) and potentially others that involve the activity of CD1d-restricted pathways in susceptible hosts at the body surfaces and perhaps elsewhere (Rossjohn et al. 2012, Nieuwenhuis et al. 2002, Lexmond et al. 2014, Leavy 2006).

Environmental and lifestyle factors have been identified as critical risk elements for development of disorders of chronic inflammation, such as IBD (Molodecky and Kaplan 2010). Consistent with this, chemical induced models of intestinal inflammation have been crucial experimental tools in investigating the pathophysiology and testing of therapeutic strategies for IBD. (Wirtz et al. 2007, Blumberg et al. 1999) Here, we have isolated the colitogenic activity within oxazolone to a five-membered heterocyclic oxazole moiety. Based on these observations, we inquired whether oxazolone is representative of a broader class of environmental factors that may be involved in the pathogenesis of IBD and possess conserved

or shared sub-structure. Oxazolone, first synthesized in 1883 by Erlenmeyer and Ploechl (Plochl 1884, Erlenmeyer 1893), has been widely utilized as a synthetic building block for compounds with a range of pharmacological properties including amino acids, antibiotics and pharmaceuticals (Kupera et al. 2011, Akram et al. 2014, Witvrouw et al. 1999, Sierra et al. 2002, Madkour et al. 2002, Khan et al. 2006, Abdel et al. 2009). Oxazole ring containing compounds are also naturally abundant in diet as a component of many thermally processed foods including roasted coffee, roasted peanuts and heated beef or as flavor enhancers such as in fish products, as well as additives to fruits and vegetables through use of pesticides and fungicides, and contained in other environmental sources such as cigarette smoke (Vitzthum et al. 1975, Stoffesima et al. 1968, Lee et al. 1981, Chang et al. 1968, Ho and Hartman 1968). Previous epidemiologic studies have attempted to explore the relationship between food intake and IBD, and have shown varying associations between coffee, peanuts, meat intake, margarine and IBD (Barthel et al. 2015, Imanzadeh et al. 2015, Eaton et al. 2015, Hou et al. 2011, Ng et al. 2015, Jowett et al. 2004). In addition, these studies have suggested that processed foods (in particular red meat and margarine) may be associated with colonic inflammation (Hou et al. 2011, Ng et al. 2015). However, dietary intake was predominantly measured from food recall diaries or weighted dietary records, and the mode of processing was not studied or discussed in detail in any of these studies. It would therefore be interesting to know if the positive associations observed were linked to oxazole-rich food compounds. The findings of our study certainly warrant more in-depth exploration of the association between intake of thermally processed, oxazole-rich foods and the incidence and prognosis of IBD as well as a variety of other allergic and inflammatory conditions that involve CD1d and NKT cells in their pathogenesis.

In addition, microbes are another abundant source of oxazoles as part of a structurally functionally diverse class of ribosomally derived peptides dubbed thiazole/oxazole modified microcins (TOMMs) generated through post-translational installation of heterocycles derived

from cysteine, serine, and threonine residues. TOMMS are widely disseminated across the phylogenetic spectra of bacterial secretion systems, including potential pathobionts associated with IBD pathogenesis or skin inflammation including *Bacteroidetes* and *Corynebacteriae*, respectively (Melby et al. 2011, Bagley et al. 2005, Vizan et al. 1991, Carvalho et al. 2012, Mukhopadhya et al. 2012). Together, this supports the convergence of environmental and microbial derived chemical structures on conserved host immune responses.

We observed that micromolar exposure to select oxazole species modulate CD1d-restricted responses in epithelial cells *in vitro* which are characterized by down-regulation of *Mttp* and reduced IL-10 production after CD1d crosslinking with NKT cell associated receptors. This mechanism has been previously shown to reduce epithelial barrier activity in response to similar concentrations of oxazolone in the colon leading to exacerbated inflammatory responses (Olzsak et al. 2014). To what degree oxazole products accumulate within the intestinal tract and the physiological concentrations and circumstances required for triggering inflammatory responses are unknown. Interestingly, at least two of the structures we identified, 2,4,5-trimethyl-1,3-dihydro-oxazole (TMO) and vinclozolin have been detected in human urine through studies associated with defining the human exposome (Table S1, Wambaugh et al. 2014). Although not directly addressed in this study, it is interesting to consider whether accumulated exposure to oxazoles derived from multifactorial sources, including diet, microbes, industry and/or agriculture acts in an additive or combinatorial manner that includes other potential non-oxazole agents in modulating host responses that are associated with disease pathogenesis.

Our gene expression profiling of intestinal epithelial cells exposed to oxazole compounds have identified a several genes (Fig 1B, 2C, 2F, 3E, S1A, S4) involved in xenobiotic metabolism and tryptophan catabolism, including indoleamine 2,3,dioxygenase 1 (IDO1), a marker highly expressed in patients suffering from IBD as well as in many animal models of colitis (Olszak et al. 2014, Barcelo-Batllori et al. 2002, Ferdinande et al. 2008, Dickgraefe et al. 2000, Wolf et al. 2004, Hansen et al. 2009). Data presented here suggest that oxazole compounds enhance the

ability of IDO1, the rate-limiting enzyme in tryptophan catabolism, to metabolize tryptophan (Fig. 5A). This supports a role for the aryl hydrocarbon receptor (AhR) as a potential cytosolic sensor or signal transducer of oxazole induced products in the intestinal epithelium (Nguyen and Bradfield 2008). Indeed, specific depletion of the AhR in the epithelium was shown to alleviate the oxazole-induced suppression of CD1d-restricted anti-inflammatory responses including production of IL-10 (Fig. 4B). Mass spectrometry analyses identified at least two products of tryptophan catabolism, kynurenic acid and xanthurenic acid, that are specifically generated in intestinal epithelial cells exposed to oxazolone or dietary and/or microbial oxazoles and their capacity to activate the AhR pathway in a manner that results in attenuation of CD1d-restricted IL-10 production. This observation is interesting given that levels of tryptophan and its byproducts in the serum have provided a robust marker for gastrointestinal pathology in clinical settings (Ciorba 2013).

In the hematopoietic system, elevated IDO1 expression and subsequent AhR activation have been associated with immune tolerance implicating this pathway in maintaining intestinal homeostasis (Apetoh et al. 2010, Li et al. 2011, Gandhi et al. 2010, Kiss et al. 2011, Bessede et al. 2014, Veldhoen et al. 2008, Qui et al. 2012). Thus loss of AhR activity in hematopoietic cells can be deleterious resulting in decreased regulatory T cells or group 3 innate like lymphoid cells that together normally restrain inflammation, maintain intestinal epithelial barrier function through production of interleukin-22 (Apetoh et al. 2010, Li et al. 2011). Similarly, both IDO1 and AhR are highly expressed within the intestinal epithelial compartment, however their role in promoting or preventing intestinal inflammation is poorly understood (Ciorba 2013, Schiering et al. 2017, Lanis et al. 2017). Here, we show that specific depletion of AhR within the intestinal epithelium, modulates CD1d-restricted responses *in vitro* and confers protection against the induction of intestinal pathology by oxazolone and a microbial oxazole compound *in vivo* (Fig. 4F, 4H). These data implicate a novel role for AhR in regulating NKT cell lipid antigen sensing

specifically in IECs, which in contrast to the effects on the hematopoietic system (Apetoh et al. 2010, Li et al. 2011), has a deleterious effect on the host in the context of colitis.

In addition, we have shown that oxazoles also downregulate MTP that is normally responsible for the loading of phospholipid antigens onto CD1d (Dougan et al. 2005, 2007). Consistent with our observations, altering MTP expression or activity has been previously shown to prevent transfer of phospholipids to CD1d or the ability of CD1d to acquire exogenous lipid antigens such as α-GC (Dougan et al. 2005). Further, loss of MTP in IECs has been shown to disable the ability of iNKT cells to induce the barrier protective cytokine, IL-10, by this cell type as we have shown previously and demonstrated here (Olszak et al. 2014). Together, our data suggest that oxazoles alter presentation of lipid auto-antigens (Fig. S1B, S1C) and exogenous lipid antigens as shown with α-GC (Fig. 1D,1E, 4C) to CD1d-restricted invariant and non-invariant NKT cells in a pathway that is dependent on AhR through the generation of tryptophan-derived metabolites. As both oxazolone and frag-oz induce inflammation in animals under GF conditions (Olszak et al. 2012, Fig. 3D-E), NKT-mediated responses to host-derived lipid antigens may be particularly important to oxazole-induced inflammation and further suggest oxazoles may thus modulate autoimmune responses to self-lipid antigens.

Conversely, it is also interesting to consider whether microbes use oxazole products to target CD1d in order to establish their niche during primary colonization potentially resulting in mucosal inflammation and pathology. Previous studies have demonstrated an important physiological role for CD1d during initial colonization of commensal and pathogenic bacteria (Nieuwenhuis et al. 2005, 2009). Specifically, CD1d-deficient animals re-derived and raised under GF conditions are unable to control colonization against gram-negative (*Pseudomonas aeruginosa, Escherichia coli*) and gram-positive (*Staphylococcus auereus, Lactobacillus gasseri*) bacteria. As a result, recently colonized CD1d-deficient GF animals exhibit an abnormal distribution of bacteria within the gastrointestinal tract and specific pathogen free, CD1d-

deficient animals exhibit an altered composition of their microbiota relative to that observed in wildtype or heterozygotic littermates (Nieuwenhuis et al. 2009). Consequently, generation of products that modulate CD1d activity such as oxazoles, which are capable of specifically inhibiting intestinal epithelial cell function may affect the ability of microbes to colonize the intestine and potentially cause inflammation.

Intestinal inflammation is often accompanied by microbial blooms, including *Enterobacteria* as compared to healthy intestine, potentially resulting in dysbiosis (Winter and Baumler Cell Microbiol. 2014, Ng et al. Nature 2013, Winter et al. Science 2013), which may be associated with production of certain microcins (Sassone-Corsi et al. Nature 2016). Interestingly, the MccB17 toxin, was initially isolated from human infants (Asensio and Perez-Diaz 1976), and delineated as an inhibitor of DNA gyrases associated with gram-positive and gram-negative microbes (Roy 1999). Further, some low molecular weight fragments of MccB17 isolated after bacterial lysis or generated by cleavage by microbial proteases retain their inhibitory activity while others lose their affinity for the MccB17 transporters, OmpF and SbmA and thus may accumulate in the intestinal lumen (Lavina J Gen. Microbiol 1986). We independently identified microcin compounds as modulators of host mediated CD1d-restricted epithelial responses based on their shared substructure with synthetic and dietary derived oxazoles. While full length MccB17 itself shared relatively low structural similarity with oxazolone, derivative products below 270Da generated either by alkaline hydrolysis or proteolytic cleavage showed relatively high similarity with both oxazolone and TMO (Table S1). Importantly we have observed that both the natural products and their synthetic analogs display similar ability to attenuate CD1d-lipid antigen presentation and subsequent CD1d-restricted IL-10 production as well as activate AhR responses specifically in IECs resulting in inflammation associated with decreased epithelial derived IL-10. That inflammation to MccB17 derivatives occurs in GF animals confirms that the effects of these compounds are directly impacting the host and not a result of their anti-microbial capacity. It is therefore intriguing to consider then

that the accumulation of oxazole compounds derived from MccB17 producing and other TOMM producing bacterial strains during a period of microbial competition may have a bystander effect on host immune responses resulting in intestinal inflammation or other effects that benefit the organism at the expense of the host.

Our data also have interesting implications for understanding the biologic mechanisms by which so-called haptens mediate their effects. Classic immunologic studies using hapten-carrier complexes have provided deep insights into concepts of B cell and T cell recognition of antigens and downstream immune responses to the hapten (e.g. oxazolone) or the protein carrier, which provides peptides for MHC class II presentation (Lemus and Karol 2008). Such pathways have been implicated in the pathogenesis of diseases such as contact hypersensitivity (Martin et al. Allergy 2011, Honda et al. J. Invest. Derm. 2013). Our studies indicate that chemical haptens may have important and direct biologic effects in their own right that could be a source of disease pathogenesis and/or modify other mechanisms. Interestingly, we have found that oxazolone conjugated to a CD1d lipid antigen, α-GC, has no effect on α-GC CD1d binding or activity *in vitro* or *in vivo* (data not shown). Such insights may have important implications for interpreting models that use other chemical haptens (Wirtz et al. 2007).

In conclusion, our studies illustrate a novel approach for interrogating triggers of inflammation due to environmental sources by searching for mimics of well-known chemical structures with established activities. In so doing, leveraging the knowledge available from oxazolone's role as a colitogenic agent via modulation of CD1d-restricted pathways we have identified oxazole containing compounds (OxC) as a new class of potential environmental agents with inflammation inducing potential that are contained within a wide range of dietary, environmental and microbial sources. With respect to the latter, our studies further show that bacterial microcins, which are well known to play a role in microbe-microbe interactions, also possess important and previously unappreciated immune regulating properties via their effects on CD1d-restricted pathways. Further, in both the case of environmental and microbial OxC we

have found that they involve epithelial sensing by the AhR, which in turn adversely affects CD1d-restricted presentation of lipid antigens that are associated with barrier protective production of IL-10. As a result, we also identified a novel pro-inflammatory activity of AhR sensing that is associated with the intestinal epithelium and have brought forth the concept that environmental triggers of inflammation that are potentially associated with IBD may function in this manner by phenocopying the activity of microbial products with similar activity.

Figure Legends

Figure 1: A minimal oxazole structure modulates expression of specific gene targets and attenuates CD1d restricted in intestinal epithelial cells leading to colonic inflammation: **A.** Panel of oxazole containing and control heterocylic natural and synthetic compounds**. B.** Relative transcript abundance in MODE-K cells stimulated with indicated compounds, normalized to β-actin**. C.** Interleukin 10 production in MODE-K cells conditioned with the indicated compounds, loaded with α-Galactosyl Ceramide (α-GC) followed by 24.7 iNKT hybridoma co-culture**. D., E.** Representative traces and quantification of surface CD1d loaded with α-GC in MODE-K cells conditioned with indicated compounds. **F.** Weight change after intra-rectal administration of 1% TMO or EtOH (50% v/v) vehicle in wildtype (WT) or CD1d-deficient (KO) animals (n=16-20)**.** *p<0.05 (Mann-Whitney U-test) **G.** Quantitative scoring for colitis after intra-rectal administration of 1% TMO or EtOH (50% v/v) vehicle in wildtype (WT) or CD1d-deficient (KO) animals (n=8). **H.** Quantification (ELISA) of Interleukin 13 and IFN-γ production from colon explants 2 days after intra-rectal administration of 1% TMO, TMC or EtOH (50% v/v) vehicle (n=3)**.** ** p<0.01 (Student's t-test). *p<0.05 **p<0.01' ***p<0.001 (Student's t-test)

Figure 2: Microbial derived oxazoles modulate CD1d restricted responses and regulate transcriptional targets in intestinal epithelial cells: Interleukin 10 response in MODE-K cells pre-conditioned with vehicle (DMSO) or indicated compounds: **A.** lysates from bacterial transformants (empty/pUC19, B17) grown in Luria Broth or M63 supplement, **B.** purified MccB17 (B17) microcin and/or B17 microcin proteolytic digest (subtilisin, trypsin), and subsequently loaded with α-GC followed by 24.7 iNKT hybridoma co-culture**. C** Relative transcript abundance of target genes, *Mttp and Ido1*, in MODE-K cells to β-actin in MODE-K pre-conditioned as in B**. D.** Panel of synthetic analogs of B17 microcin proteolysis products with indicated anti-microbial activity. **E.** Interleukin 10 response in MODE-K cells pre-conditioned with vehicle, oxazolone, or synthetic MccB17 microcin analogs, and subsequently loaded with

α-GC followed by 24.7 iNKT hybridoma co-culture. **F.** Relative transcript abundance of target genes in MODE-K cells to β-actin in MODE-K pre-conditioned as in E**. ***p<0.05; **p<0.01; ***p<0.001 (Student's t-test).

Figure 3: NKT cells are required for colonic inflammation induced by Frag-oz: A. Quantitative scoring for colitis after intra-rectal administration of 1% TMO or EtOH (50% v/v) vehicle in wildtype (WT) or CD1d-deficient (KO) littermates (n=8). **B.** Quantification of Interleukin 13 and IFN-γ production in overnatant of colon explants 2 days after intra-rectal administration of 1% TMO or EtOH (50% v/v) vehicle (n=6) **C.** Weight change after intra-rectal administration of 1% Frag-oz or EtOH (50% v/v) vehicle in Germ Free or specific pathogen free animals (n=8)**. ****p<0.01; ***p<0.001 (Mann-Whitney U-test). Quantification of **D.** *Mttp* and **E.** *Cyp1a1* transcripts (normalized to β-actin) from mucosal scraping 2 days after intra-rectal administration of 1% Frag-oz, or EtOH (50% v/v) vehicle (n=4)**.** **p<0.01; ***p<0.001 (Student's t-test) **F.** Quantitative scoring for colitis after intra-rectal administration of 1% TMO or EtOH (50% v/v) vehicle in germ free or specific pathogen free animals (n=8-9)**. ****p<0.01; p<0.001 (Student's t-test).

Figure 4: Activation of Aryl Hydrocarbon Receptor by dietary and microbial derived oxazole compounds: A. Aryl Hydrocarbon Receptor promoter-reporter activity after MODE-K cells conditioned with indicated compounds. MODE-K cells transfected with scrambled (solid fill) or siRNA targeted against AhR (clear fill), conditioned with indicated compounds and then loaded with α-GC followed by 24.7 iNKT hybridoma co-culture **B.** Interleukin 10 production. **C.** Quantification of surface CD1d loaded with α-GC. **D.** Quantification of Interleukin 10 from overnatant of colon explants 3 days after intra-rectal administration of 1% oxazolone or 1% Frag-oz EtOH (50% v/v) vehicle in WT or animals with AhR-deficiency in epithelial compartment ($Ahr^{\Delta IEC}$). (n=4)**.** Weight change after intra-rectal administration of **E.** 1% oxazolone or EtOH (50% v/v) vehicle or **G.** 1% Frag-oz or EtOH (50% v/v) vehicle in WT or animals with AhR-

deficiency in epithelial compartment ($Ahr^{\Delta IEC}$). *** p<0.001 (Mann-Whitney U-test) **F, H.** Quantitative scoring for colitis after intra-rectal administration of oxazolone (F) or frag-oz (H) in EtOH (50% v/v) in WT or animals with AhR-deficiency in epithelial compartment ($Ahr^{\Delta IEC}$) (N=5-10). *p<0.05; ** p<0.01; ***p<0.001 (Student's t-test).

Figure 5: Oxazoles induce the generation of tryptophan derived metabolites that attenuate epithelial CD1d-restricted responses in an AhR dependent manner: A. Recombinant IDO1 was incubated with L-tryptophan in the presence of oxazole (oxazolone, TMO, Frag-oz), control (TMC) compounds or vehicle and formyl-kynurenine production measured via a calorimetric assay, **B.** MODE-K cells cultured with L-tryptophan deficient media or media supplemented with exogenous L-tryptophan and CD1d-restricted Interleukin 10 responses measured in MODE-K cells pre-conditioned with vehicle or indicated compounds. **C**. LC-MS quantification of label retaining metabolites in MODE-K cells grown under tryptophan deficient conditions and supplemented with deuterated tryptophan and conditioned with the indicated compounds. **D.** CD1d-restricted Interleukin 10 responses in MODE-K cells pre-conditioned with vehicle or oxazolone in tryptophan deficient media with supplementation with L-tryptophan, DL-methyl tryptophan, kynurenine, kynurenic acid, or xanthurenic acid and then loaded with α-GC followed by 24.7 iNKT hybridoma co-culture**. E.** CD1d-restricted Interleukin 10 production by MODE-K cells transfected with scrambled (solid fill) or siRNA targeted against AhR (clear fill) in tryptophan deficient media. CD1d-restricted Interleukin 10 responses were measured following pre-conditioning with vehicle, TMC, oxazolone, TMO or frag-oz with or without supplementation of L-tryptophan or kynurenic acid. ***p<0.001 (Student's t-test).

Figure 6. Exposure to environmental oxazoles (from diet or microbes) influences CD1d-restricted responses in intestinal epithelial cells through production of tryptophan derivatives that activate the aryl hydrocarbon receptor pathway. Intestinal epithelial cells (IEC) promote mucosal barrier protection through microsomal triglyceride protein (MTP)

mediated CD1d-restricted production of Interleukin 10 (IL-10, blue circles). Upon exposure to oxazole compounds (derived from diet, microbes or other environmental sources), these CD1d-restricted responses are attenuated through a mechanism involving the production of tryptophan derived metabolites (kynurenic acid, xanthurenic acid, orange squares), through the activity of IDO1, that trigger the aryl hydrocarbon receptor (AhR). Decreased, CD1d-restricted IL-10 production results in unrestrained inflammatory responses (IL-13/IFNγ, red dots) and resulting pathology. ER (endoplasmic reticulum), IFN-γ (Interferon γ).

Author Contribution

Conceptualization S.S.I., T.G. and R.S.B. Methodology, S.S.I., T.G., A.G., S.F.O., F.C., C.S., A.L., A.M., and R.S.B. Analysis S.S.I., T.G., A.G., S.F.O, F.C., A.L., A.M., and R.S.B. Writing and Editing S.S.I., T.G., A.G., P.D., R.B.S., G.B., R.H., A.L., A.M., and R.S.B.

Acknowledgements

R.S.B. is supported by NIH grant DK044319, DK053056, DK051362, DK088199, 5P01AI073748 and the Harvard Digestive Diseases Center (P30DK034854). S.I and T.G is supported by Crohn's and Colitis Foundation of America Research Fellow Award (383527, 418509). We thank Drs. Roberto Kolter and Dennis Kasper (Harvard Medical School) for reagents and discussion of data, Drs. Keith Houck and Jill Franzosa (Environmental Protection Agency) for helpful discussions and Toxcast21 data, and Vladimir Yeliseyev and Marla Marquez for technical assistance. We thank Amanjot Riar and Blumberg laboratory members for assistance in manuscript preparation.

STAR Methods

Contact for Reagent and Resource Sharing

Further information and requests of reagents can be directed to and fulfilled by the Lead Contact, Dr. Richard S. Blumberg (BLUMBERG@BWH.HARVARD.EDU).

Experimental Model and Subject Details

Animals

Mice (C57Bl/6J) were housed in a specific pathogen-free (SPF) barrier facility at Harvard Medical School: Wildtype, *Ahr*$^{fl/fl}$, Villin-Cre, mice were purchased from The Jackson Laboratory. *Ahr*$^{-/-}$ mice were purchased from Taconic USA and maintained as heterozygotes. *Cd1d1*$^{-/-}$*Cd1d2*$^{-/-}$ have been described (Exley et al. 2003). Animal studies were conducted in a gender and age matched (8-10 week) manner using littermates for each experiment, except for wildtype versus *Cd1d*$^{-/-}$ comparisons. SPF and Germ-free animals were bred and maintained in vinyl isolators in the Harvard Digestive Disease Center Gnotobiotic and Microbiology Core. For colitis experiments, mice were transferred to Optimice cages (Animal Care Systems) for daily monitoring under sterile conditions. All procedures were approved by the Harvard Medical Area Standing Committee on Animals.

Primary Cultures

Bone marrow derived cells (BMDC) were purified from mouse femurs and cultured for 7 days in RPMI (supplemented with 10% fetal bovine serum, 1% antibiotic-antimycotic, Gibco and 20 ng/mL granulocyte-macrophage colon-stimulating factor, Biosource). For primary hepatocyte isolation, mice were anesthetized with intraperitoneal injection of ketamine (87 mg/kg body weight) plus xylazine (13 mg/kg body weight), after which the inferior vena cava was exposed, cannulated and perfused for 5 min with liver perfusion media (Invitrogen), followed by a 10 min perfusion with liver digestion media (Invitrogen). The digested liver was minced in hepatocyte

was media (Invitrogen) and cells were pelleted and resuspended in Williams E medium (10% FBS, 10^{-7}M dexamethasone, 10 μg/ml insulin and 5 μg/ml transferrin.

Bacterial Stocks and Purification

MccB17 was generated and purified as described (Collin et al. 2013, Li et al. 1996). Plasmid pUC19, wild-type or carrying the complete biosynthetic operon (*mcbABCDEFG*), was transformed into competent DH5α or MG1655 *E. coli*.

Synthesis of Microcin B17 and Derivatives

Overnight colonies were grown in LB media and used to inoculate M63 media (3 g/l KH_2PO_4, 7 g/l K_2HPO_4, 2 g/l $(NH_4)SO_4$, 1 mM $MgSO_4$, 1 μg/ml thiamine, 0.2% glucose, 0.1 mg/ml ampicillin) or LB Media (0.1mg/mL ampicillin) and incubated for 48 h. Cells were pelleted and lysed in a boiling solution of 1 mM EDTA and 100 mM acetic acid. Cellular debris was removed by centrifugation, protein was quantified by BCA Assay kit (ThermoFisher Scientific) according to manufacturer's instructions and lysates were serially titrated (1μg-10μg/mL) incubated with MODE-K cells for co-culture assays as described. Digestion of full length MccB17 (a gift from A. Maxwell, Collin et al. 2013) by subtilisin (Sigma) (0.1 mM MccB17, 10% DMSO, 10 mM NaAcO, 5 mM $Ca(AcO)_2$) or sequence grade trypsin (Promega) (0.5 mM 50 μg/mL trypsin, 1%DMSO in buffer (Promega) for 24 h to completion (Collin et al. 2013). Entire digested products (or equivalent buffer with enzyme) was then incubated with MODE-K cells for co-culture and qPCR analyses.

Synthesis of Frag-oz

Frag-oz, frag-tz, frag-oztz, and frag-tzoz originally were kindly provided by R. Payne, School of Chemistry University of Sydney or later synthesized by A.L. The compounds were synthesized according to established procedures for microcin B17-related oxazole and thiazole synthesis (Videnov et al. 1996).

Refer to Figure S6A. Step 1. Synthesis of 2-(aminomethyl)oxazole-4-carboxamide (Fig S6A) *Tert*-butyl ((4-carbamoyloxazol-2-yl)methyl)carbamate 1[1] (0.895 g, 3.71 mmol) was stirred in TFA/CH_2Cl_2 (1:1 v/v, 40 mL) at room temperature for 1 h. The solvent was removed under reduced pressure affording the title compound as a brown oil (0.367g, 70%). ^{1}H NMR (400 MHz, Methanol-d_4) δ 8.42 (s, 1H), 4.28 (s, 2H). Step 2. 2-(acetamidomethyl)oxazole-4-carboxamide (Frag-oz): To a solution of 2-(aminomethyl)oxazole-4-carboxamide **2** (630mg, 4.46 mmol) in DMF (2.2 mL) at 0ºC TEA (0.7 mL, 4.9 mmol) was added followed by Acetyl Chloride (0.35 mL, 4.9 mmol). The solution was stirred for 5 h at 0ºC. The DMF was removed under reduced pressure and the crude product was purified by column chromatography on silica [DCM-Methanol, 9:1 (v/v)] affording the title compound as a white solid (400mg, 49%). ^{1}H NMR (400 MHz, Methanol-d_4) δ 8.30 (s, 1H), 4.48 (s, 2H), 1.99 (s, 3H). ^{13}C NMR (101 MHz, Methanol-d_4) δ 172.12 , 163.71 , 161.52 , 142.01 , 135.76 , 35.87 , 20.92.

***Tert*-butyl ((4-carbamoylthiazol-2-yl)methyl)carbamate (4)**

Aqueous ammonia (28% w/w, 3,1 mL, 40 mmol) was added to a solution of ethyl 2-(((*tert*-butoxycarbonyl)amino)methyl)thiazole-4-carboxylate[2] 3 (381 mg, 1.33 mmol) in methanol (1,3 mL). After 16 h at 45ºC, the reaction mixture was concentrated affording the title compound as a brown oil (315mg, 92%) which was used directñy in the next step. ^{1}H NMR (400 MHz, Methanol-d_4) δ 8.10 (s, 1H), 4.49 (s, 2H), 1.45 (s, 9H).

2-(aminomethyl)thiazole-4-carboxamide (5)

Tert-butyl ((4-carbamoylthiazol-2-yl)methyl)carbamate **4** (0.342 g, 1.331 mmol) was stirred in TFA/CH_2Cl_2 (1:1 v/v, 13 mL) at room temperature for 1.5 h. The solvent was removed under reduced pressure affording the title compound as a green oil (0.150, 72%) which was used directly in the next step. ^{1}H NMR (400 MHz, Methanol-d_4) δ 8.25 (s, 1H), 4.41 (s, 2H).

Synthesis of Frag-tz 2-(acetamidomethyl)thiazole-4-carboxamide

Refer to Fig. S6B. To a solution of 2-(aminomethyl)thiazole-4-carboxamide **5** (204mg, 1.30 mmol) in DMF (6.5mL) at 0ºC, Triethylamine (TEA , 0.2 mL, 1.43 mmol) was added followed by

Acetyl Chloride (0.1 mL, 1.43 mM). The solution was stirred for 5 h at 0ºC. The solvent was removed

under reduced pressure and the crude product was purified by column chromatography on silica [CH_2Cl_2 /Methanol, 9:1 (v/v)] affording the title compound as a white solid (80mg, 31%). ^{1}H NMR (400 MHz, Methanol-d_4) δ 8.11 (s, 1H), 4.63 (s, 2H), 2.01 (s, 3H). ^{13}C NMR (101 MHz, Methanol-d_4) δ 172.13 , 169.43 , 164.11 , 149.10 , 124.41 , 40.47 , 21.01.

Method Details

Experimental colitis model

For reciprocal sensitization studies (Fig. S3), mice were pre-sensitized by epicutaneous application of 3% w/v oxazolone (4-ethoxymethylene-2-phenyl-2-oxazolin-5-one, Sigma-Aldrich) or 2,4,5-trimethyl-2,5-dihydro-1,3-oxazole (Sigma-Aldrich) in 100% ethanol (200 □L volume). Five days later, animals were re-challenged intra-rectally (through a 3.5F catheter) with 1% vehicle, oxazolone or 2,4,5-trimethyl-2,5-dihydro-1,3-oxazole in 50% ethanol (5 □L/g of body weight) as indicated. For all other studies, vehicle, oxazolone, 2,4,5-trimethyl-2,5-dihydro-1,3-oxazole, 1,2,4-trimethylcyclopentane (Sigma-Aldrich) were administered intra-rectally (through a 3.5F catheter) as a 1% solution in 50% ethanol (5 μl/g of body weight). Body weight, rectal bleeding, and stool consistency were analyzed 1-2 times daily. Tissues obtained at the indicated time points were embedded in paraffin, stained with hematoxylin and eosin, and examined by a pathologist (Dr. Jon Glickman) in a blinded fashion for evidence of colitis according to five established criteria: mononuclear inflammation, crypt hyperplasia, epithelial injury, neutrophilic inflammation, and hypervascularization grading on 4 point scale (0=absent, 1=mild, 2=moderate, 3=severe).

Colon organ culture

Standardized segments (1 cm × 1 cm) of the transverse colon were washed in cold PBS supplemented with penicillin and streptomycin (GIBCO) and cultured in 24-well flat-bottom

culture plates (Falcon) in RPMI 1640 media (GIBCO) for 24 h at 37°C. Supernatants were analyzed for cytokines IL-10, IL-13 and IL-1β by ELISA (all BD).

Cells and Antigen presentation assays

1 x 10^5 BMDCs, primary hepatocytes or 0.5 x 10^5 MODE-K cells (Vidal et al. 1993) were incubated in 96 well plates (Corning) maintained in RPMI (supplemented with 2% fetal bovine serum, 1% antibiotic-antimycotic, Gibco) were pulsed with the indicated compounds dissolved in dimethyl sulfoxide (DMSO) at a concentration of 10 □M for 36-48h. Cells were washed three times with sterile phosphate buffered saline (PBS, Gibco) after which cells were incubated with 100 ng ml^{-1} alpha-galactosyl ceramide/KRN7000 or beta-glucosyl ceramide (Avanti Polar Lipids) for 3h, washed three times with sterile PBS, before addition of 2 x 10^4 NKT hybridoma cells including 24.7, 24.8, and 14S6 overnight co-culture after which supernatant was collected and clarified by centrifugation. Mouse IL-10, IFN□ production was assessed by ELISA (OptEIA, BD Biosciences). For aryl hydrocarbon receptor siRNA mediated knockdown, MODE-K cells were transfected with AM100441, AM 100360, or Silencer negative control siRNAs (ThermoFisher Scientific) using Lipofectamine 2000 (Life Technologies) according to manufacturer's instructions. AhR silencing was verified 48h after transfection by quantitative polymerase chain reaction.

Identification of Tryptophan Derived Metabolites

MODE-K cells were cultured in dialyzed FBS and RPMI (Gibco #26400044, RPMI 1640 cGMP #100001229, all amino acids <1nM,) and supplemented with essential amino acids (histidine, isoleucine, leucine, lysine, methionine, phenylalanine, threonine, and valine at 1μM) and supplemented with deuterated tryptophan (1 μM D5-Trp, Santa Cruz sc-391262, see Key Resources Table). Lysates were extracted from cell pellets in 80% Methanol and analyzed with reverse phase HPLC-MS (Agilent C18 column connected with Thermo Scientific LTQ-XL, see Key Resources Table).

IDO1 enzymatic assay

Recombinant His-tagged IDO1 was incubated with 10nM concentrations of TMC, oxazolone, TMO, or frag-oz and assay was performed according to the manufacturer's instruction (BPS Bioscience, San Diego, CA, see Key Resources Table)

CD1d and CD1d-lipid complex measurements by flow cytometry.

MODE-K cells were pulsed with 10 μM indicated compounds dissolved in DMSO for 36-48h. Cells were washed three times with sterile PBS after which cells were incubated with 100 ng ml^{-1} alpha-galactosyl ceramide/KRN7000 or the non-agonistic compound, beta-glucosyl ceramide (data not shown), for 3 h, washed three times with sterile PBS. Cells were lifted in 10 mM EDTA/PBS and stained with the following antibodies: mouse L363 (eBiosciences, see Key Resources Table), mouse CD1d (BD Bioscience, see Key Resources Table). For intracellular staining, cells were fixed using the Intracellular Fixation and Permeabilization Buffer Set (eBioscience, see Key Resources Table) according to the manufacturer's instructions. Flow cytometry was performed on MACSQuant Analyzer (Miltenyi Biotec) and analyzed using FlowJo software.

Quantitative polymerase chain reaction assays

RNA samples were prepared using an RNeasy Mini Kit and cDNAs were synthesized using the Omniscript RT Kit (Qiagen, see Key Resources Table). Real-time RT–PCR was performed using SYBR Green I Master Mix (Roche) and a CFX96 Real-Time System (Bio-Rad, see Key Resources Table). Values were normalized to β-actin (see Key Resources Table).

Luciferase promoter-reporter assays

For aryl hydrocarbon receptor luciferase assays, MODE-K cells were cultured on 6-well plates (Corning). pGL4.43 Luc2pXRE (Promega) or empty pGL4.43 (Promega) and 100 ng Renilla luciferase (Promega) was transfected into MODE-K cells using Lipofectamine 2000. Twenty four hours later, MODE-K cells were conditioned with indicated compounds for 48 h. Cells were

lysed and firefly luciferase (normalized to renilla luciferase) was measured using Dual Luciferase Reporter Assay System (Promega)

In-silico similarity screening

We used two-step in-silico screening process. First, broad similarity screening was performed to identify oxazole related natural compounds from various databases including Pubchem, Super Natural II a database of natural products (Bannerjee et al. 2015), Dictionary of natural products Chemnet database, and The Human Metabolome Database (Wishart et al. 2013) (Table S1). Second, focused screen search was performed based on the results of first screening to identify natural compounds related to a 5-membered oxazole ring of oxazolone with emphasis to find minimal structural features of oxazolone for its inflammatory activity. This focused screen selection was based on identification of natural compounds with Tanimoto similarity of more than 0.5 and/or Euclidean distance scores cutoff of 0.9 (Table S1). Natural compounds were queried in the standard SMILES format. Tanimoto similarities between compounds were computed with the Chemmine Similarity Workbench, which calculated maximum common substructure (MCS) similarities with the Tanimoto coefficient (Cao et al. 2008). Euclidean distance scores were calculated using Noncontiguous atom matching structural similarity function (NAMS) (Teixeira et al. 2013). The following formulas were used to calculate MCS similarity and TS score of natural compounds with Oxazolone and Oxazole ring substituted with a methyl group at the 2, 4 and 5 position. MCS similarity score: Atom number (AN) in MCS/AN in smaller molecule TS similarity score: AN in MCS/ (AN in smaller molecule + AN in larger molecule –AN in MCS). Based on the results of the screening process, 2,5-Dihydro-2,4,5-trimethyloxazole (TMO) with Tanimoto/Euclidean similarity score of 0.78/0.97 was selected as one of the natural compound for *in vivo* experiments. To further investigate the role of nitrogen and oxygen atoms of the oxazole ring and correlate them with colitogenic activity, Trimethylcyclopentane (TMC) and 2-Methyl-1-pyrroline (1MP) were selected as additional

controls. In addition, Vinclozolin was selected based on Euclidean distance score of 0.94 and widespread fungicide usage.

Supplementary Figures

Figure S1 (Refers to Figure 1). A minimal oxazole structure modulates intestinal epithelial transcriptional and antigen presentation capacity to invariant and non-variant NKT cells. **A.** Relative transcript abundance in MODE-K cells conditioned with the indicated compounds, normalized to β-actin. **p<0.01 (Student's t-test). B. CD1d-restricted Interleukin 10 production in the absence of exogenous lipid supplementation in MODE-K cells conditioned with the indicated compounds followed by co-culture with **B.** invariant NKT (24.8) or **C.** non-invariant NKT (14S.6) hybridomas. ***p<0.001 (Student's t-test). **D.** Interferon γ production in bone marrow derived dendritic cells conditioned with the indicated compounds followed by loading with α-galactosyl ceramide and co-cultured with 24.7 iNKT hybridoma.

Figure S2 (Refers to Figure 1): A minimal oxazole structure does not alter CD1d protein expression or cellular distribution: Quantification of surface and intra-cellular CD1d protein expression in MODE-K cells conditioned with the indicated compounds for 48hr, as measured by **A.** flow cytometry and, **B.** relative proportions of intracellular and cell surface CD1d protein abundance.

Figure S3 (refers to Figure 3): Intestinal inflammation, epithelial response and pathology to oxazole containing compounds does not require apriori host sensitization. A. Representative sections of wildtype animals administered 1% of the indicated compounds (50% EtOH v/v) by intra-rectal challenge and analyzed by H&E stain after 3 days. 10X magnification, scale bar (40 μM). Quantification of **B.** *Mttp* and **C.** *Cyp1a1* transcripts (normalized to β-actin) from mucosal scrapings 2 days after intra-rectal challenge with 1% TMO, 1% TMC or EtOH

(50%v/v) vehicle (n=3). *p<0.05, ***p<0.001 (Student's t-test). **D.** Animals were sensitized by topical application of the indicated compounds followed by intra-rectal administration of 1% TMO, 1% oxazolone, or EtOH (50% v/v) vehicle in wildtype C57Bl/6 animals. Quantitative colitis scoring was assessed on colons harvested 3 days after intra-rectal challenge. ***p<0.001 (Student's t-test).

Figure S4 (refers to Figure 4): Aryl hydrocarbon receptor mediates expression of a subset of gene targets in response to oxazole containing compounds: MODE-K cells transfected with control or AhR specific siRNA, conditioned with the indicated compounds and relative transcript abundance was measured normalized to β-actin. **A.** *cyp1a1*, **B.** *Ido1*, **C.** *Mttp* ***p<0.001 (Student's t-test).

Figure S4 (refers to Figure 4): Aryl hydrocarbon receptor attenuates CD1d-restricted responses in primary hepatocytes: Interleukin 10 production from primary hepatocytes derived from WT or AhR-deficient (KO) animals were conditioned with the indicated compounds, loaded with α-galactosyl ceramide followed by co-culture with 24.7 iNKT hybridoma. *** p<0.001 (Student's t-test).

Figure S5 (Refers to STAR Methods): Synthesis of Frag-oz and Frag-tz.

Figure 1

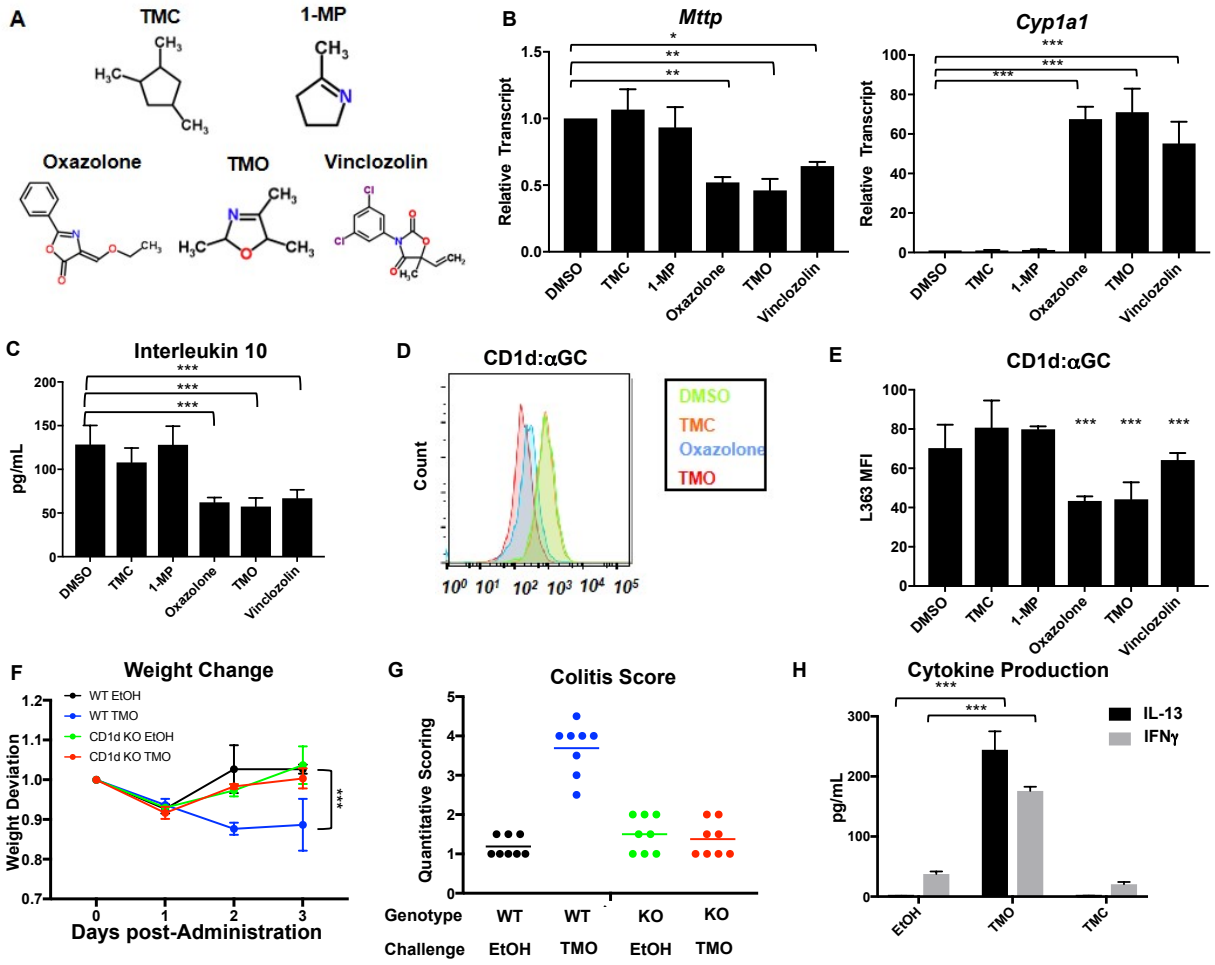
A
TMC
1-MP
Oxazolone
TMO
Vinclozolin
B
Mttp
Relative Transcript
DMSO
TMC
1-MP
Oxazolone
TMO
Vinclozolin
Cyp1a1
Relative Transcript
C
Interleukin 10
pg/mL
D
CD1d:αGC
Count
DMSO
TMC
Oxazolone
TMO
E
CD1d:αGC
L363 MFI
F
Weight Change
WT EtOH
WT TMO
CD1d KO EtOH
CD1d KO TMO
Weight Deviation
Days post-Administration
G
Colitis Score
Quantitative Scoring
Genotype
WT
WT
KO
KO
Challenge
EtOH
TMO
EtOH
TMO
H
Cytokine Production
IL-13
IFNγ
pg/mL
EtOH
TMO
TMC

Figure 2

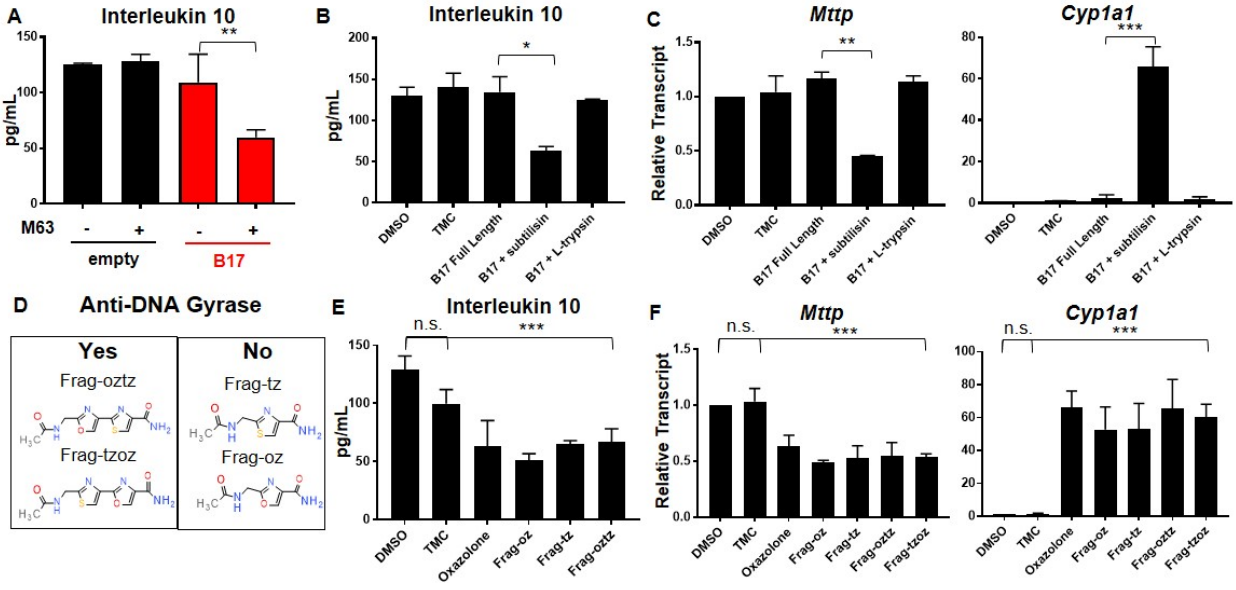
A
Interleukin 10
pg/mL
M63
empty
B17
B
Interleukin 10
pg/mL
DMSO
TMC
B17 Full Length
B17 + subtilisin
B17 + L-trypsin
C
Mttp
Relative Transcript
Cyp1a1
D
Anti-DNA Gyrase
Yes
Frag-oztz
Frag-tzoz
No
Frag-tz
Frag-oz
E
Interleukin 10
n.s.
pg/mL
Oxazolone
Frag-oz
Frag-tz
Frag-oztz
F
Mttp
Cyp1a1
Relative Transcript
Frag-tzoz

Figure 3

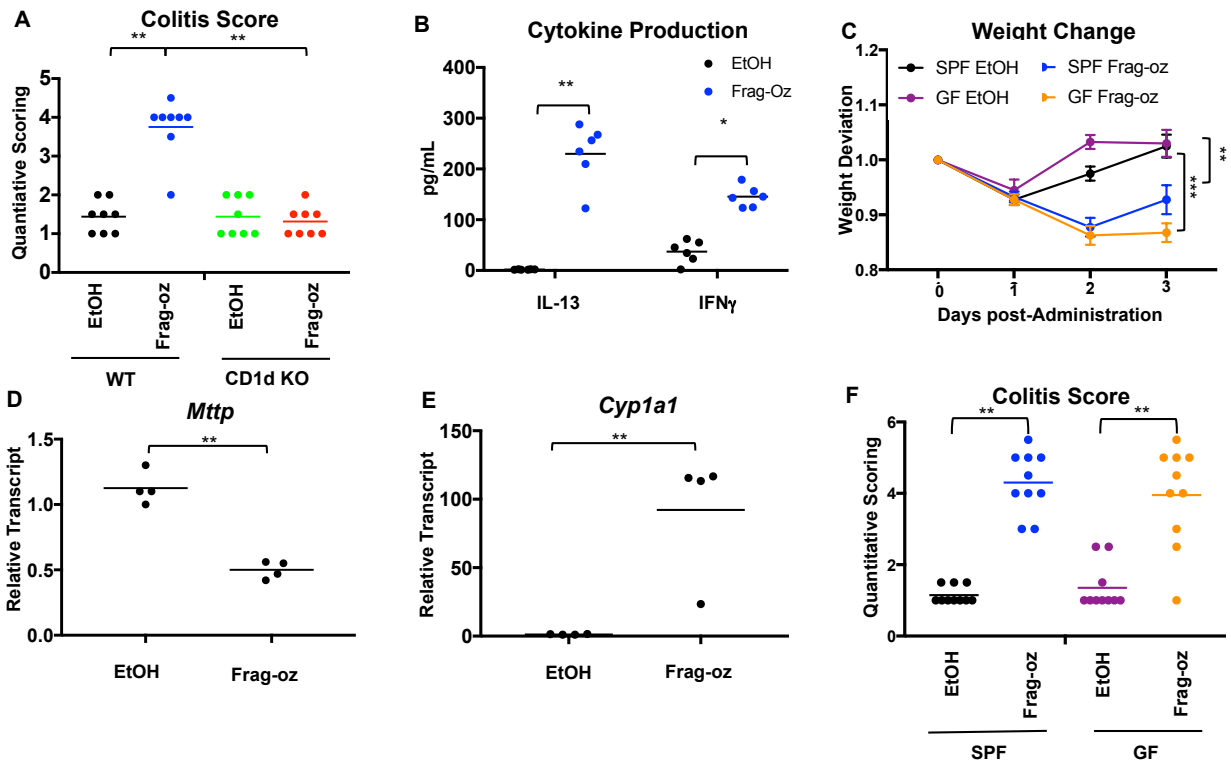
A
Colitis Score
Quantitative Scoring
EtOH
Frag-oz
EtOH
Frag-oz
WT
CD1d KO
B
Cytokine Production
pg/mL
EtOH
Frag-Oz
IL-13
IFNγ
C
Weight Change
SPF EtOH
SPF Frag-oz
GF EtOH
GF Frag-oz
Weight Deviation
Days post-Administration
D
Mttp
Relative Transcript
EtOH
Frag-oz
E
Cyp1a1
Relative Transcript
EtOH
Frag-oz
F
Colitis Score
Quantitative Scoring
EtOH
Frag-oz
EtOH
Frag-oz
SPF
GF

Figure 4

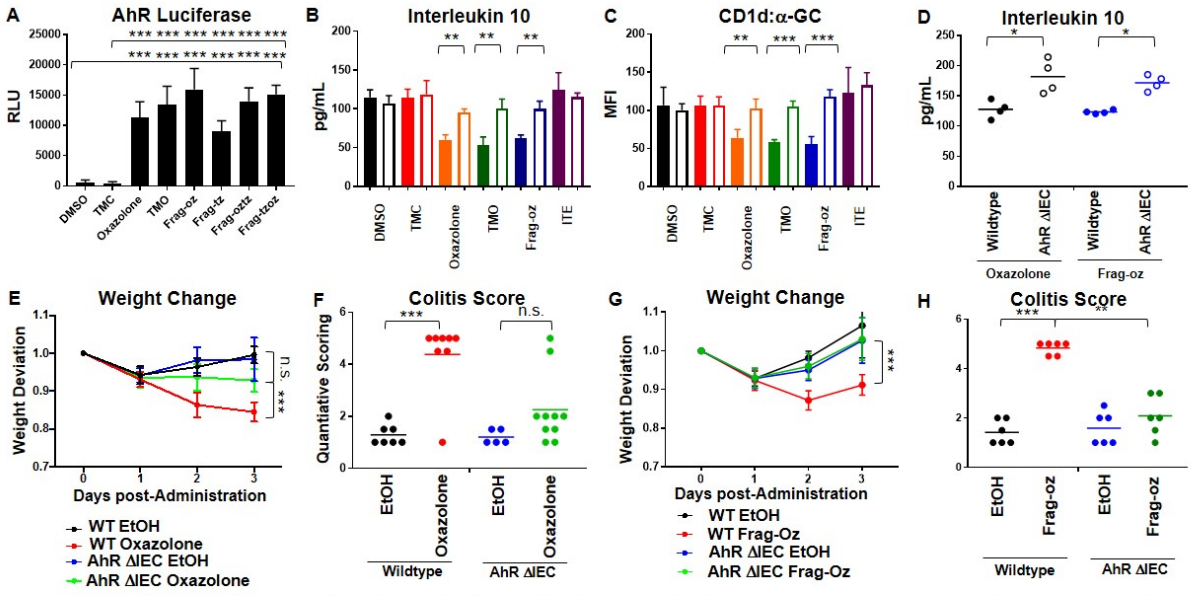
A
AhR Luciferase
RLU
DMSO
TMC
Oxazolone
TMO
Frag-oz
Frag-tz
Frag-oztz
Frag-tzoz
B
Interleukin 10
pg/mL
DMSO
TMC
Oxazolone
TMO
Frag-oz
ITE
C
CD1d:α-GC
MFI
DMSO
TMC
Oxazolone
TMO
Frag-oz
ITE
D
Interleukin 10
pg/mL
Wildtype
AhR ΔIEC
Wildtype
AhR ΔIEC
Oxazolone
Frag-oz
E
Weight Change
Weight Deviation
Days post-Administration
n.s.
***
WT EtOH
WT Oxazolone
AhR ΔIEC EtOH
AhR ΔIEC Oxazolone
F
Colitis Score
Quantiative Scoring
***
n.s.
EtOH
Oxazolone
EtOH
Oxazolone
Wildtype
AhR ΔIEC
G
Weight Change
Weight Deviation
***
Days post-Administration
WT EtOH
WT Frag-Oz
AhR ΔIEC EtOH
AhR ΔIEC Frag-Oz
H
Colitis Score
***
**
EtOH
Frag-oz
EtOH
Frag-oz
Wildtype
AhR ΔIEC

Figure 5

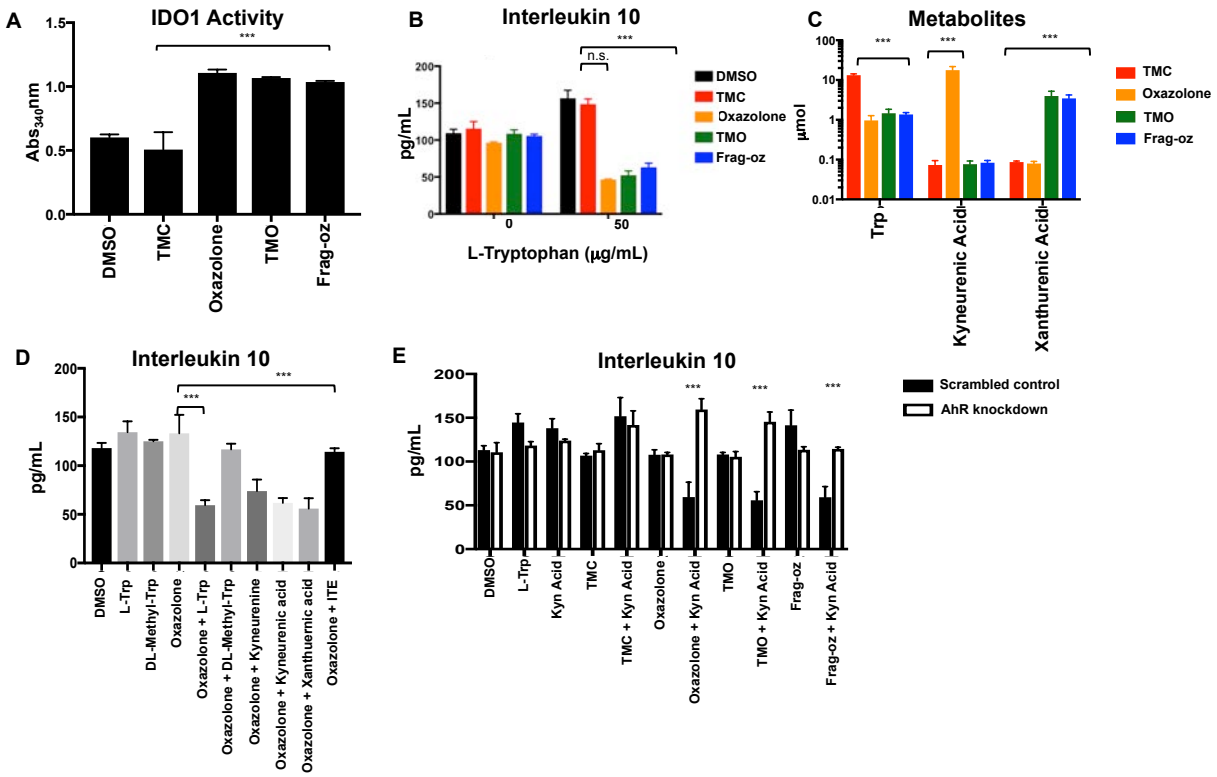
A
IDO1 Activity
Abs340nm
DMSO
TMC
Oxazolone
TMO
Frag-oz
B
Interleukin 10
pg/mL
n.s.
L-Tryptophan (µg/mL)
C
Metabolites
µmol
Trp
Kyneurenic Acid
Xanthurenic Acid
D
Interleukin 10
pg/mL
DMSO
L-Trp
DL-Methyl-Trp
Oxazolone
Oxazolone + L-Trp
Oxazolone + DL-Methyl-Trp
Oxazolone + Kyneurenine
Oxazolone + Kyneurenic acid
Oxazolone + Xanthuernic acid
Oxazolone + ITE
E
Interleukin 10
pg/mL
Kyn Acid
TMC + Kyn Acid
Oxazolone + Kyn Acid
TMO + Kyn Acid
Frag-oz + Kyn Acid
Scrambled control
AhR knockdown

Figure 6

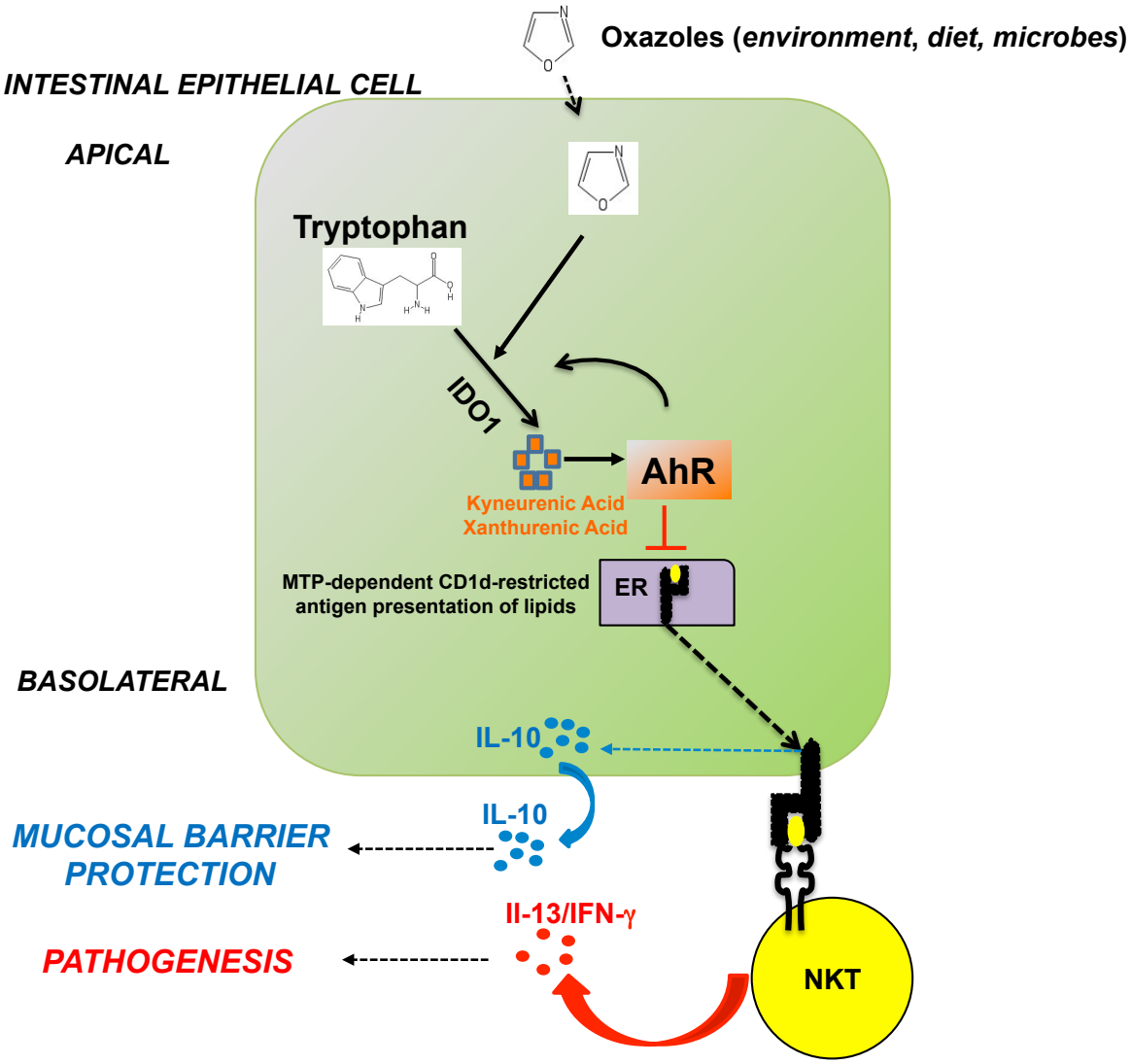
Oxazoles (environment, diet, microbes)
INTESTINAL EPITHELIAL CELL
APICAL
Tryptophan
IDO1
AhR
Kyneurenic Acid
Xanthurenic Acid
MTP-dependent CD1d-restricted antigen presentation of lipids
ER
BASOLATERAL
IL-10
IL-10
MUCOSAL BARRIER PROTECTION
Il-13/IFN-γ
PATHOGENESIS
NKT

Figure S1

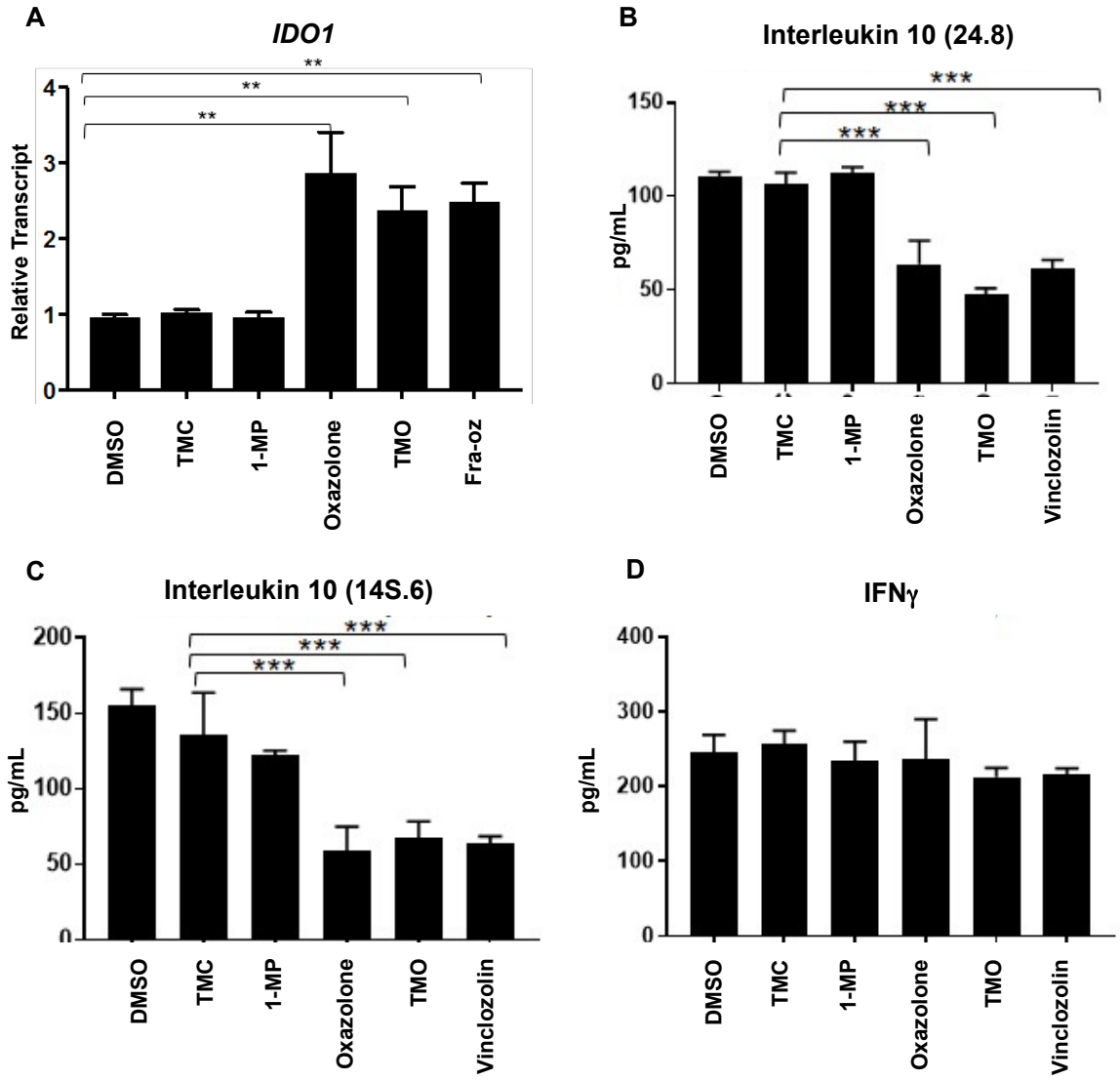
A
IDO1
Relative Transcript
0
1
2
3
4
**
**
**
DMSO
TMC
1-MP
Oxazolone
TMO
Fra-oz
B
Interleukin 10 (24.8)
pg/mL
0
50
100
150
***
***
***
DMSO
TMC
1-MP
Oxazolone
TMO
Vinclozolin
C
Interleukin 10 (14S.6)
pg/mL
0
50
100
150
200
***
***
***
DMSO
TMC
1-MP
Oxazolone
TMO
Vinclozolin
D
IFNγ
pg/mL
0
100
200
300
400
DMSO
TMC
1-MP
Oxazolone
TMO
Vinclozolin

Figure S2

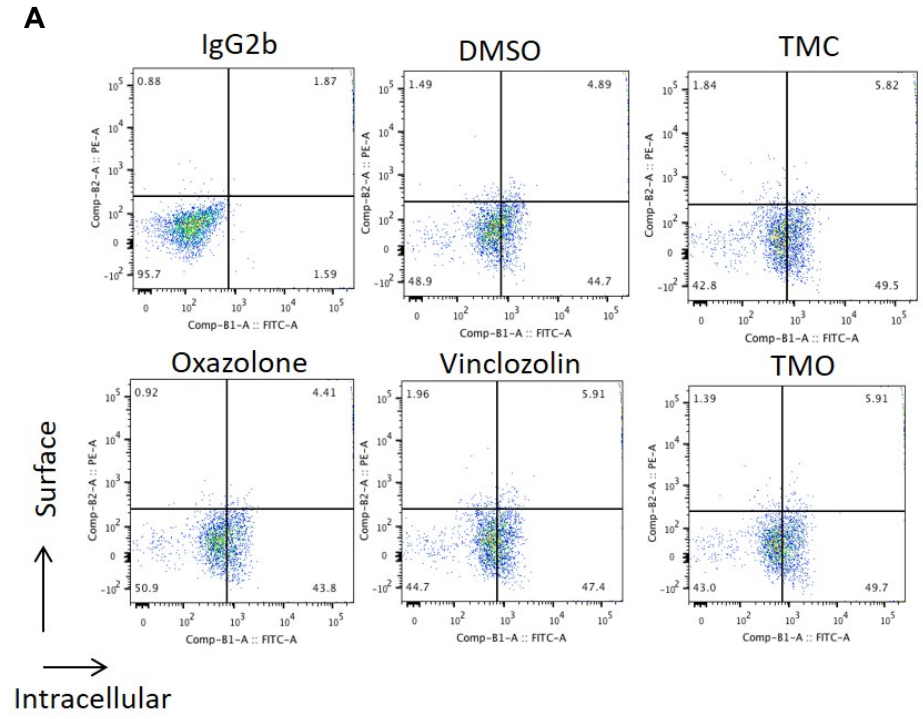
A
IgG2b
DMSO
TMC
Oxazolone
Vinclozolin
TMO
Surface
Intracellular
Comp-B2-A :: PE-A
Comp-B1-A :: FITC-A
0.88
1.87
95.7
1.59
1.49
4.89
48.9
44.7
1.84
5.82
42.8
49.5
0.92
4.41
50.9
43.8
1.96
5.91
44.7
47.4
1.39
5.91
43.0
49.7

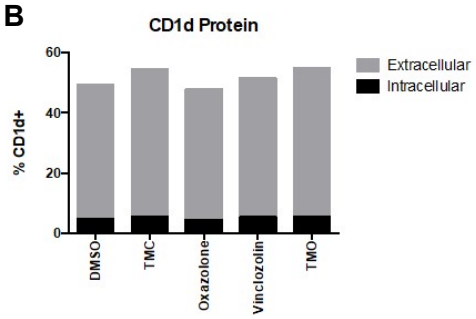
B
CD1d Protein
% CD1d+
Extracellular
Intracellular
DMSO
TMC
Oxazolone
Vinclozolin
TMO

Figure S3

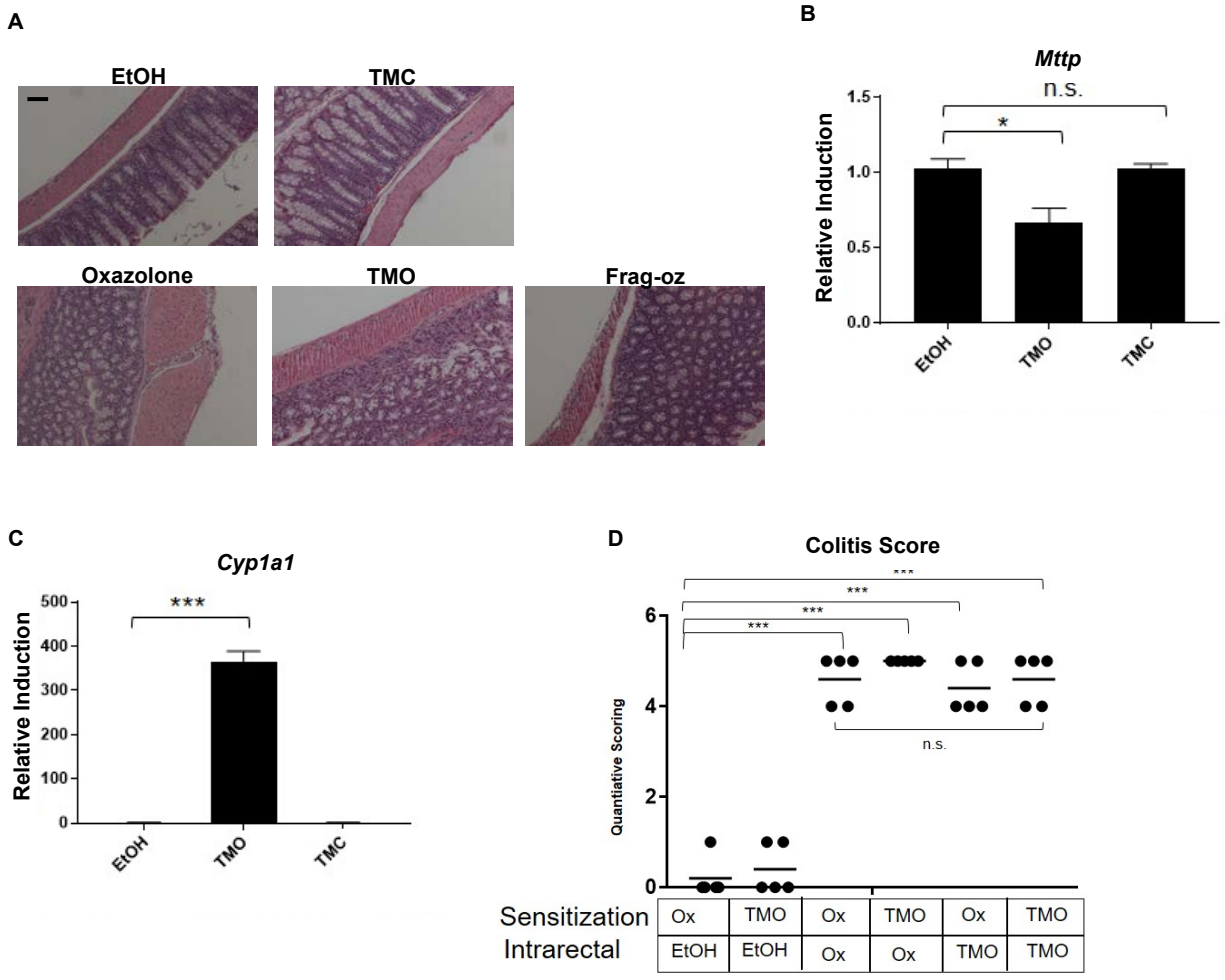
A
EtOH
TMC
Oxazolone
TMO
Frag-oz
B
Mttp
n.s.
*
Relative Induction
1.5
1.0
0.5
0.0
EtOH
TMO
TMC
C
Cyp1a1
***
Relative Induction
500
400
300
200
100
0
EtOH
TMO
TMC
D
Colitis Score
***
***
***
***
Quantiative Scoring
6
4
2
0
n.s.
Sensitization
Intrarectal
Ox
TMO
Ox
TMO
Ox
TMO
EtOH
EtOH
Ox
Ox
TMO
TMO

Figure S4

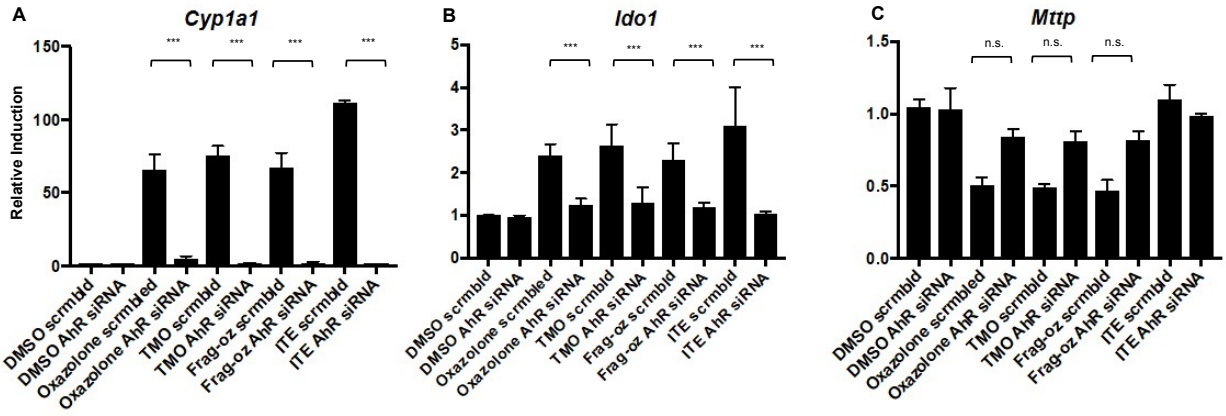

Figure S5

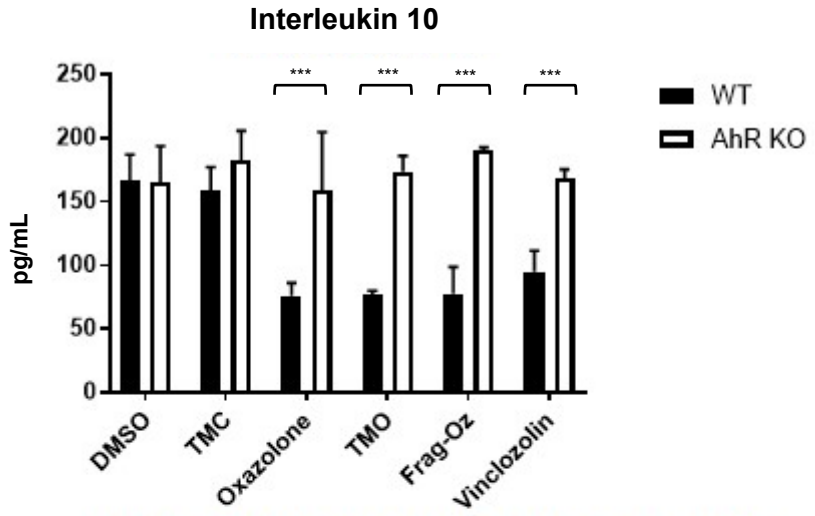

Figure S6

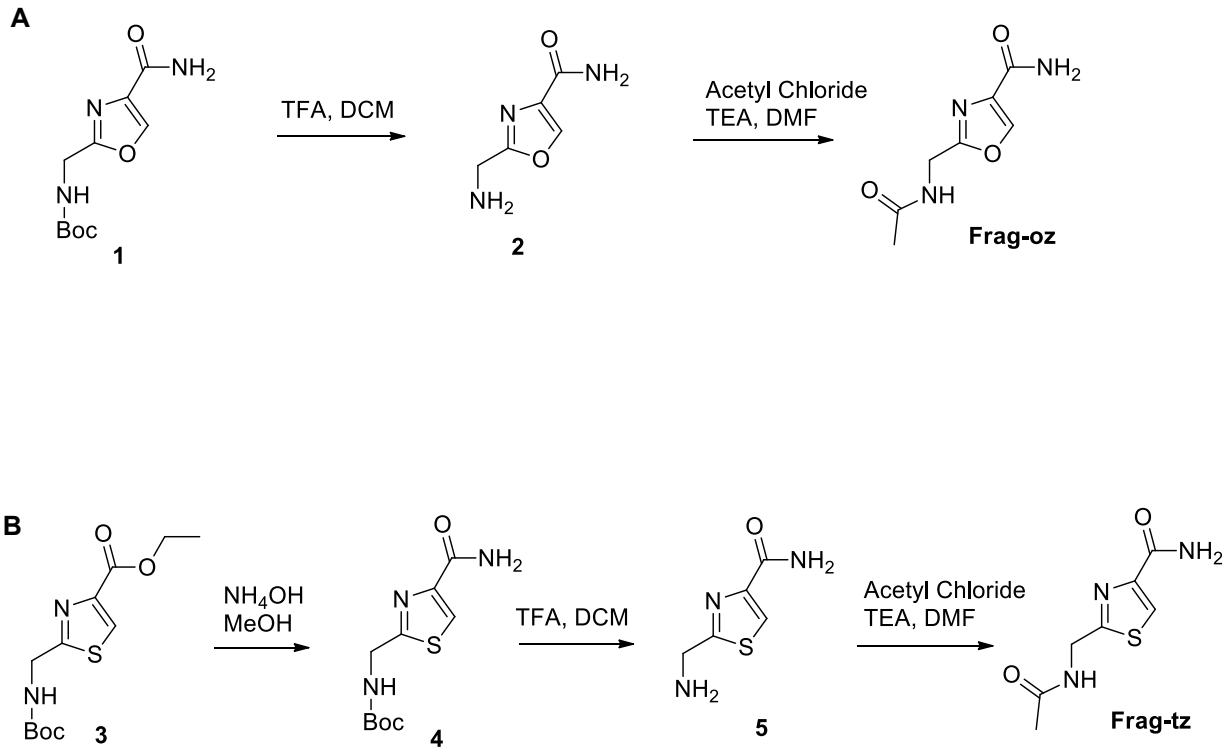
A
TFA, DCM
Acetyl Chloride
TEA, DMF
Boc
1
2
Frag-oz
B
NH4OH
MeOH
TFA, DCM
Acetyl Chloride
TEA, DMF
3
4
5
Frag-tz

Table S1: Oxazole-like structures identified by in silica screen against three chemical databases of naturally occurring compounds (Human Metabolome Database, Super Natural II database, Dictionary of Natural Compounds (Banerjee et al. 2015, Wishart et al 2007) using 3 parameters: Maximum Common Structure (MCS Similarity), Tanimoto similarity (Tc Similarity, Euclidean Distance Score.

Chemical Name	CAS/ Chemspider ID (C	Database	MCS Similarity		Tc Similarity		Euclidean Distance Score		
Column1	Column2	Column3	With Oxazolone	With 5-Membered Oxazole Ring	With Oxazolone4	With 5-Membered Oxazole Ring5	With Oxazolone6	With 5-Membered Oxazole Ring7	Source
2-Oxazolidinethione	2015027 (CID)	Dictionary of natural products	0.67	0.67	0.22	0.4	0.94	0.97	Food
4-Oxazolol	9882770 (CID)	Dictionary of natural products	0.83	0.83	0.29	0.56	0.95	0.98	N.A.
4,5-Dihydro-2-(2-hydroxyphenyl)-4-oxazolecarboxylic acid	13459647 (CID)	Dictionary of natural products	0.73	0.87	0.55	0.44	0.96	0.96	N.A.
4,5-Dihydro-2,5-diphenyloxazole	9588301 (CID)	Dictionary of natural products	0.69	0.87	0.5	0.39	0.95	0.97	N.A.
Aerucyclamide A	23342203 (CID)	Dictionary of natural products	0.44	1	0.14	0.18	0.86	0.88	Microbes
Agrobactin	20130128 (CID)	Dictionary of natural products	0.69	1	0.21	0.17	0.89	0.94	Microbes
Allosamidin	106593 (CID)	Dictionary of natural products	0.37	0.87	0.1	0.11	0.91	0.95	Microbes
Almazolone	10481088 (CID)	Dictionary of natural products	0.56	0.75	0.28	0.23	0.93	0.93	Microbes
Amychelin	28289083 (CID)	Dictionary of natural products	0.69	0.87	0.17	0.12	0.89	0.94	Microbes
Amythiamicin A	172053 (CID)	Dictionary of natural products	0.69	0.87	0.13	0.09	0.82	0.83	Microbes
Anachelin	10215353 (CID)	Dictionary of natural products	0.69	0.87	0.17	0.12	0.86	0.91	Microbes
Ascidiacyclamide	143441 (CID)	Dictionary of natural products	0.5	1	0.11	0.13	0.88	0.9	Microbes
Carboxymycobactin T	4883340 (C ID)	Dictionary of natural products	0.62	0.75	0.16	0.1	0.9	0.91	Microbes
Cladioxazole	10192495 (CID)	Dictionary of natural products	0.31	0.87	0.15	0.3	0.94	0.98	Microbes
Comoramide B	8684204 (CID)	Dictionary of natural products	0.44	0.87	0.1	0.12	0.88	0.9	Microbes
Cycloxazoline	140316 (CID)	Dictionary of natural products	0.44	1	0.12	0.17	0.92	0.95	Microbes
Didmolamide A	8432198 (CID)	Dictionary of natural products	0.5	1	0.16	0.19	0.88	0.9	Microbes
Dolastatin I	8273575 (CID)	Dictionary of natural products	0.5	0.87	0.16	0.17	0.85	0.87	Microbes
Fluvibactin	20129583 (CID)	Dictionary of natural products	0.69	1	0.21	0.17	0.89	0.94	Microbes
Indolmycin	182220 (CID)	Dictionary of natural products	0.44	0.75	0.23	0.25	0.91	0.94	Microbes
Leupyrrin C	10208508 (CID)	Dictionary of natural products	0.62	1	0.16	0.14	0.9	0.9	Microbes
Lissoclinamide 1	10355731 (CID)	Dictionary of natural products	0.5	1	0.12	0.14	0.86	0.88	Microbes
Mycobactin P	4952811 (CID)	Dictionary of natural products	0.44	0.87	0.1	0.11	0.88	0.89	Microbes
Nagelamide R	29214003 (CID)	Dictionary of natural products	0.62	0.87	0.18	0.14	0.87	0.88	Microbes
Nigribactin	29215280 (CID)	Dictionary of natural products	0.69	0.87	0.23	0.16	0.94	0.94	Microbes
Nocardichelin A	23284472 (CID)	Dictionary of natural products	0.68	0.87	0.19	0.13	0.89	0.93	Microbes
Oxachelin	28283771 (CID)	Dictionary of natural products	0.68	0.87	0.22	0.55	0.89	0.94	Microbes
Patellamide A	138571 (CID)	Dictionary of natural products	0.5	1	0.11	0.13	0.88	0.9	Microbes
Prepatellamide A	29212979 (CID)	Dictionary of natural products	0.5	0.87	0.12	0.11	0.87	0.9	Microbes
Raocyclamide A	9094062 (CID)	Dictionary of natural products	0.5	0.75	0.15	0.13	0.85	0.87	Microbes
Serratiochelin A	35523320 (CID)	Dictionary of natural products	0.68	1	0.29	0.24	0.94	0.94	Microbes
Shahidine	28285985 (CID)	Dictionary of natural products	0.68	0.87	0.4	0.3	0.94	0.96	Microbes
Spoxazomicin A	28288733 (CID)	Dictionary of natural products	0.68	0.87	0.35	0.26	0.89	0.94	Microbes
Ulicyclamide	8230874 (CID)	Dictionary of natural products	0.5	1	0.13	0.15	0.86	0.88	Microbes
Ulithiacyclamide	10263374 (CID)	Dictionary of natural products	0.5	1	0.12	0.14	0.87	0.89	Microbes
Vibriobactin	4575382 (CID)	Dictionary of natural products	0.44	0.75	0.11	0.1	0.89	0.89	Microbes
1-Hydroxy-3-methyl-9H-carbazole	14960-81-7 (CAS)	Human Metabolome	0.43	0.5	0.28	0.2	0.93	0.95	Food
2-Ethyl-4,5-dimethyloxazole	53833-30-0 (CAS)	Human Metabolome	0.78	0.75	0.39	0.54	0.92	0.94	Food
2-Isobutyl-4,5-dimethyloxazole	26131-91-9 (CAS)	Human Metabolome	0.63	0.75	0.35	0.46	0.91	0.94	Food
2,4-Dimethyloxazole	7208-05-1 (CAS)	Human Metabolome	0.86	0.86	0.35	0.67	0.92	0.95	Food
2,5-Dihydro-2,4-dimethyloxazole	77311-02-5 (CAS)	Human Metabolome	0.85	0.85	0.35	0.67	0.94	0.97	Food
2,5-Dimethyloxazole	23012-11-5 (CAS)	Human Metabolome	0.71	0.85	0.28	0.67	0.92	0.95	Food
4-Ethyl-5-methyl-2-(1-methylethyl)oxazole	84027-96-3 (CAS)	Human Metabolome	0.63	0.75	0.35	0.46	0.91	0.94	Food
4-Ethyl-5-methyl-2-propyloxazole	84027-94-1 (CAS)	Human Metabolome	0.63	0.75	0.35	0.46	0.91	0.94	N.A.
4,5-Dimethyl-2-(1-methylethyl)oxazole	19519-45-0 (CAS)	Human Metabolome	0.7	0.75	0.37	0.5	0.92	0.94	Food
4,5-Dimethyl-2-propyloxazole	53833-32-2 (CAS)	Human Metabolome	0.7	0.75	0.37	0.5	0.91	0.94	Food
4,5-Dimethyloxazole	20662-83-3 (CAS)	Human Metabolome	0.71	0.71	0.28	0.5	0.92	0.95	Food
5-Ethyl-4-methyl-2-(1-methylethyl)oxazole	102586-54-9 (CAS)	Human Metabolome	0.63	0.75	0.35	0.46	0.91	0.94	Food
5-Ethyl-4-methyloxazole	29584-92-7 (CAS)	Human Metabolome	0.62	0.62	0.26	0.45	0.92	0.95	Food
Methylhalfordinol	33864-03-8 (CAS)	Human Metabolome	0.68	0.75	0.46	0.29	0.91	0.92	Food
Trimethyloxazole	20662-84-4 (CAS)	Human Metabolome	0.75	0.75	0.33	0.6	0.92	0.95	Food
2,5-Dihydro-2,4,5-trimethyloxazole	22694-96-8 (CAS)	Human Metabolome/Toxcast	0.75	0.87	0.33	0.78	0.94	0.97	Food
(4E)-2-phenyl-4-(phenylmethylidene)-1,3-oxazol-5-one	4648348 (CID)	Super Natural II	0.75	0.75	0.52	0.28	0.97	0.93	N.A.
(4E)-4-(3-Hydroxybenzylidene)-3-phenyl-1,2-oxazol-5(4H)-one	1376002 (CID)	Super Natural II	0.5	0.5	0.28	0.17	0.97	0.91	N.A.
(4E)-4-(naphthalen-1-ylmethylidene)-2-phenyl-1,3-oxazol-5-one	1266836 (CID)	Super Natural II	0.81	0.75	0.5	0.24	0.97	0.95	N.A.
(4E)-4-[(2,4-dimethylphenyl)methylidene]-	601096 (CID)	Super Natural II	0.81	0.75	0.54	0.26	0.97	0.95	N.A.
(4E)-4-[(4-{[(4Z)-5-oxo-2-phenyl-1,3-oxazol-4-ylidene]methyl}phenyl)methylidene]-2-phenyl-1,3-oxazol-5-one	1645167 (CID)	Super Natural II	0.81	0.75	0.37	0.17	0.97	0.95	Food
(4E)-4-[(4-bromophenyl)methylidene]-2-phenyl-1,3-oxazol-5-one	1266410 (CID)	Super Natural II	0.81	0.75	0.56	0.27	0.97	0.95	N.A.
(4E)-4-[(4-ethoxyphenyl)methylidene]-2-phenyl-1,3-oxazol-5-one	583707 (CID)	Super Natural II	0.81	0.75	0.52	0.25	0.96	0.95	N.A.
(4E)-4-[(4-methoxyphenyl)methylidene]-2-phenyl-1,3-oxazol-5-one	600847 (CID)	Super Natural II	0.81	0.75	0.54	0.26	0.97	0.95	N.A.
(4E)-4-[(4-methylphenyl)methylidene]-2-phenyl-1,3-oxazol-5-one	617653 (CID)	Super Natural II	0.81	0.75	0.56	0.27	0.97	0.95	N.A.
2-phenyl-4-(propan-2-ylidene)-1,3-oxazol-5-one	300575 (CID)	Super Natural II	0.8	0.87	0.63	0.43	0.98	0.97	N.A.
4-(anthracen-9-ylmethylidene)-2-phenyl-	1424197 (CID)	Super Natural II	0.81	0.75	0.43	0.2	0.97	0.95	N.A.
Vinclozolin	36278 (CID)	Toxcast	0.37	0.62	0.21	0.24	0.91	0.94	Agriculture
Microcin B17	58107855 (CID)	Synthesized for manuscript	0.5	0.75	0.03	0.02			Microbes
Frag-oz		Synthesized for manuscript	0.54	0.75	0.32	0.4	0.91	0.93	Microbes/Synthetic
Frag-tz		Synthesized for manuscript	0.54	0.62	0.32	0.32	0.9	0.93	Microbes/Synthetic